Metrologia

PAPER

Impact of the latest generation of Josephson voltage standards in ac and dc electric metrology

IOP Publishing | Bureau International des Poids et Mesures Metrologia

Metrologia 55 (2018) S152–S173 https://doi.org/10.1088/1681-7575/aad41a

Impact of the latest generation of Josephson voltage standards in ac and dc electric metrology

Alain Rüfenacht, Nathan E Flowers-Jacobs and Samuel P Benz

National Institute of Standards and Technology, Boulder, CO 80305, United States of America

E-mail: alain.rufenacht@nist.gov

Received 8 May 2018, revised 7 July 2018
Accepted for publication 18 July 2018
Published 24 August 2018

Abstract

For decades, the quantum behavior of Josephson junctions has been employed as intrinsic standards for voltage metrology. Conventional dc Josephson voltage standards have been the primary standards for voltage, programmable Josephson voltage standards have been implemented in calibration services and precision measurements, such as the Planck constant, and Josephson arbitrary waveform synthesizers have been employed in ac voltage calibrations and precision measurements of the Boltzmann constant. With the anticipated redefinition of the Système International d'Unités, all types of Josephson voltage standards will become intrinsic standards and equivalent realizations of the unit volt. Here we review the state-of-the art performance, best practices, and current impact of these systems for various applications, with an emphasis on ac voltage metrology. We explain the limitations of each system, especially regarding the many potential systematic errors that affect their accuracy and performance for specific applications.

Keywords: digital-to-analog conversion, Josephson junction arrays, measurement standards, signal synthesis, superconducting integrated circuits, voltage measurement, Josephson voltage standard

(Some figures may appear in colour only in the online journal)

1. Introduction

The discovery of the Josephson effect [1] and the subsequent development of the first Josephson voltage standards led to dramatic improvements in the accuracy of primary dc voltage references. The first steps in the evolution of quantum-based voltage standards were achieved in the 1970s, first with a circuit containing a single Josephson junction and then with array circuits that produced increasingly larger dc output voltages by successively adding more junctions in series to the arrays. By the late 1980s the output voltage of conventional Josephson voltage standard (CJVS) array circuits reached the practical value of 10 V, starting a broad international dissemination of Josephson voltage standards among National Metrology Institutes (NMIs) and many primary calibration laboratories (see [2, 3] for reviews of CJVS technology and early Josephson based voltage standards). The second leap forward was achieved in the mid 1990s with the successful design and fabrication of large arrays of Josephson junctions (JJs) with metallic barriers [4, 5], instead of the insulating barrier used with CJVS. The non-hysteretic electrical properties of the metallic barrier circuits produced quantized voltages that were intrinsically stable and accurate over a large range of bias current, thus enhancing their stability to external current perturbations.

Two complementary types of Josephson voltage standards used today are the programmable Josephson voltage standard (PJVS) and the Josephson arbitrary waveform synthesizer (JAWS, also known as the ac Josephson voltage standard or ACJVS). The accuracy of all Josephson voltage standard systems, including the CJVS, PJVS, and JAWS systems, relies upon the ac Josephson effect, in which the voltage across a junction is precisely proportional to the rate of change of the phase difference between the junction's two superconducting

electrodes. When a junction is biased with a periodic current of appropriate amplitude and frequency such as continuous microwaves or periodic pulses, the superconducting phase difference responds synchronously, and the junction produces synchronized, voltage pulses with quantized area over a range of dc bias current. The generated voltage pulses are governed by the ac Josephson equation, which depends only on two fundamental constants of nature: the Planck constant h and the elementary charge (equal to the absolute value of the electron charge) e. With the upcoming redefinition of the Système International d'Unités (SI), the value of these two fundamental constants will be fixed [6, 7]. As a result, in 2019 Josephson voltage standards will become a direct realization of the unit volt, rather than a 'representation of the volt' based on the values of e and h adopted in 1990. After the SI redefinition, the realization of the unit volt can be independently achieved in every calibration laboratory, assuming the frequency standard used to lock the bias current pulse repetition rate of the Josephson voltage standard is linked to an SI-traceable time base.

The first generation of CJVS-type Josephson voltage standards, with zero-current crossing steps, is still widely used by many NMIs and is currently the primary voltage standard for their dc voltage calibrations. However, over the past few years a number of CJVS systems have been replaced by PJVS systems. Besides their intrinsic stability and rapid programmability, PJVS systems have the additional capability of generating programmable ac reference waveforms from dc to a few kilohertz for use in ac voltage and power metrology applications. Direct dc comparison between PJVS and CJVS systems have demonstrated agreement of 1 part in 10^{10} or better at 10 V [8, 9] and direct comparison of two PJVS systems has demonstrated agreement better than 1 part in 10^{11} [10]. Thus, the replacement of CJVS systems with PJVS systems will have no impact on reported calibration accuracy.

Quantum voltage standards are, in principle, intrinsically accurate. However, this statement is valid only over a finite range of bias and environmental parameters. The quantum locking ranges[1] of both PJVS and JAWS systems must be periodically verified during regular calibration procedures to ensure they are performing as quantum standards with their expected accuracy. An understanding of, and routine checking for, all systematic errors (e.g. the effect of leakage current and inductive errors for the JAWS), and implementation best practices for each measurement setup, are critical for successful operation of Josephson voltage standards in metrology applications.

Currently, traceability for ac voltage is based exclusively on ac–dc thermal voltage converters (TVCs) [11]. Unlike dc voltage metrology that relies on accurate reference sources, the use of TVCs for ac metrology is a 'detector-based' approach. In general, measurements with TVCs are time-consuming and require multiple detectors to cover the voltage and frequency domain. Recent increases in the output voltage of JAWS standards [12–14] could greatly simplify the realization of accurate ac voltages and will enable direct comparisons of commercial sources. In addition, calibration with JAWS standards could potentially reduce overall measurement uncertainty, measurement duration, and the extensive overhead of maintaining and calibrating numerous transfer standards in the calibration chain.

In this review article, we present the best practices for implementing JAWS and PJVS systems in both dc and ac metrology applications. We discuss the advantages and challenges associated with the change from a 'detector-based' to 'source-based' ac voltage metrology. Such implementation will also require periodic verification of the equivalence of the disseminated Josephson voltage standards.

[1] The quantum locking range is the range of bias over which every Josephson junction in an array produces a single voltage pulse per input bias pulse (see section 3.1).

2. Josephson voltage standards

A properly operating Josephson voltage standard exploits the perfect frequency-to-voltage conversion of the Josephson effect in junctions formed by a weak link (or barrier) between two superconductors. The effect that describes this conversion was discovered by Josephson [1], and the quantized voltages produced by a junction when biased at microwave frequencies were first experimentally observed by Shapiro [15].

When biased with a current pulse of appropriate magnitude and width, a Josephson junction generates a voltage pulse with a quantized time-integrated area exactly equal to the inverse Josephson constant $K_J^{-1} = h/2e$ (the magnetic flux quantum), that is, the ratio of two fundamental constants. In PJVS systems, the combination of an ac current bias with frequency f (typically >10 GHz) and a dc current bias results in a signed integer number n of quantized voltage pulses per ac period and produces a dc voltage V given by

$$V = n \times M \times K_J^{-1} \times f,$$

where M is the number of JJs in series. In JAWS systems, the JJs are biased by a fast pulse generator that controls the pulse pattern to generate a low-frequency waveform with the output voltage determined precisely by the known pulse sequence.

Until May 2019, all Josephson voltage standards will continue to represent the unit volt by use of the value of K_J defined in 1990 ($K_{J\text{-}90} = 483\ 597.9$ GHz V^{-1}) [16]. After the redefinition, the new value will be

$$K_J = 2e/h = 483\ 597.848\ 416\ 984\ldots \text{ GHz V}^{-1},$$

based on the following exact values of e and h [17]:

$$e = 1.602\ 176\ 634 \times 10{-}19\,\text{C}, \text{ and}$$

$$h = 6.626\ 070\ 15 \times 10^{-34}\,\text{J} \cdot \text{s}.$$

Note that with the transition to the new SI value of K_J, all secondary voltage standards will see a discontinuity of -1.07 parts in 10^7 in their calibration values.

2.1. Programmable Josephson voltage standards

A PJVS system programs the output voltage by biasing various segments of the series-connected Josephson array circuit with various predefined dc bias currents (see [18, 19] for details). To achieve proper operation, this programmable array circuit requires long arrays of uniform JJs with uniformly applied

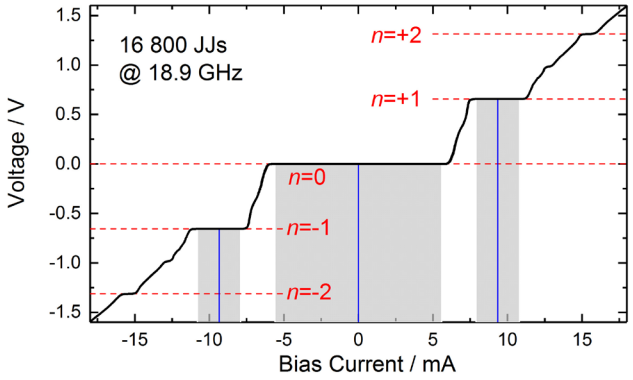

Figure 1. Typical *V–I* curve characteristic of a 16 800 JJ segment (MSB) measured on a 10 V PJVS circuit. The voltage is accurately defined on the $n = 0$, $n = +1$, and $n = -1$ constant voltage steps, but only over the bias current range shown in the grayed areas. The optimum bias value of each step (0 mA, +9.3 mA and −9.3 mA for $n = 0$, $+1$, and -1, respectively) is indicated by a blue vertical line. The $n = \pm 2$ constant voltage steps are visible, but the bias current range is too small to be reliably operated (<1 mA).

microwave bias along the whole array. Compared to CJVS systems, the main advantages of PJVS systems are the large milliampere operating current range, the rapid programmability, and the intrinsic stability of the selected output voltage. A disadvantage of PJVS systems is that the electronics providing the dc bias currents are always connected to the PJVS circuit, resulting in multiple leakage current paths to ground (Earth). The PJVS bias electronics and circuit wiring must be properly designed to minimize leakage current contributions so they do not cause significant systematic errors.

To achieve the best voltage resolution, a PJVS circuit is subdivided into segments or subarrays, each containing a definite number of JJs. Initially the number of JJs for the shorter segments were distributed in a binary sequence (multiple of: 1, 2, 4, 8, 16, …) [20, 21]. However, to take full advantage of the three bias states ($n = 0$, $n = +1$ and $n = -1$) of the PJVS voltage–current (*V–I*) characteristic (figure 1), a distribution of the JJs in a ternary sequence (multiple of: 1, 3, 9, 27, 81, …) is a much more efficient option that minimizes the number of bias channels without compromising the resolution [22]. This method can easily be extended to a quinary sequence of JJs (multiple of: 1, 5, 25, 125, 625, …) if future performance of PJVS circuits allows simultaneous operation of the five steps $n = +2$, $+1$, 0, -1 and -2.

The segment with the smallest number of JJs is called the least significant bit (LSB). Sometimes more than one large segment or most significant bit (MSB) is required in the PJVS circuit to maximize circuit performance and to attain the largest output voltages. Because their values depend on temperature, applied microwave power and frequency, the bias current range of all subarrays must be experimentally measured with a digital voltmeter (DVM). The circuit performance is optimized by selecting the midpoint of the range for the bias values for each voltage of each segment (these values are typically collected in a current-bias or current-margins table).

The present JJ technology used at the National Institute of Standards and Technology (NIST) and the Physikalisch–Technische Bundesanstalt (PTB) is based on superconducting/normal metal barrier/superconducting (SNS) junctions made of Nb/Nb_xSi_{1-x}/Nb [23]. The National Metrology Institute of Japan (NMIJ) and the National Institute of Advanced Industrial Science and Technology (AIST) have developed NbN/TiN_x/NbN SNS junctions for their PJVS circuits, which can be operated at higher temperatures (up to 11 K) compared to niobium-based junctions (typically <5 K). Although operation at higher temperatures allows use of smaller cryogenic coolers, the fabrication process for NbN-based junctions, requiring epitaxial growth, is more challenging.

NMIJ/AIST, PTB, and NIST have all developed PJVS circuits capable of reaching dc output voltages of at least 10 V. The NIST 10 V PJVS circuit has 265 116 JJs biased at a selectable frequency between 18.3 GHz and 22 GHz [18, 24]. The junctions are distributed in 32 parallel coplanar waveguides (CPWs), and uniform microwave power is delivered to each of the 32 CPWs by use of Wilkinson dividers made with lumped-element superconducting circuits [25]. The Wilkinson dividers suppress microwave reflections at each branch that can negatively affect microwave power uniformity along the array and circuit performance. The NIST circuits also use impedance tapering of the CPWs, typically from 50 Ω to ~30 Ω, which allows a more uniform distribution of microwave current across all JJs in a given CPW [26]. To make the circuits more compact, the junctions are stacked vertically in groups of three [27], as shown in the scanning electron microscope (SEM) image in figure 2. Such vertical integration is required to reach a density of more than a quarter million JJs over a 12 mm × 17 mm surface area.

The PTB circuit design is based on 128 parallel micro-strip microwave transmission lines and is optimized for frequencies of around 70 GHz. Its main advantage is that it requires only 69 632 single-stacked JJs to reach 10 V [28, 29]. The same circuit design is implemented with the 10 V PJVS system commercially available from Supracon AG[2]. PTB has realized a PJVS circuit with an output voltage of 20 V by adding an additional JJ in a vertical stack (double stack) to their single-stacked 10 V circuit design, effectively doubling the number of JJs in the circuit [30].

With 524 288 JJs, the NMIJ/AIST circuit is at present the most complex PJVS device to reach a voltage of at least 10 V (figure 3). Operated at 16 GHz, it can achieve an output voltage of 17 V when all segments are biased in the $n = +1$ state. By containing redundant JJs, this design can accommodate circuits with minor defects, thereby increasing the number of NbN-based circuits capable of reaching 10 V [31, 32]. However, achieving high-yield fabrication processes for PJVS circuits having several hundred thousand JJs is a challenging task [33, 34]. Double-stacked JJs are incorporated in the 17 V design, and the microwave distribution uses a 64-way splitter. NMIJ/AIST is currently developing a new design of 'serial-parallel' power dividers [35] for future Josephson voltage standard circuits.

[2] Certain commercial equipment, instruments, or materials are identified in this paper to facilitate understanding. Such identification does not imply recommendation or endorsement by NIST, nor does it imply that the materials or equipment that are identified are necessarily the best available for the purpose.

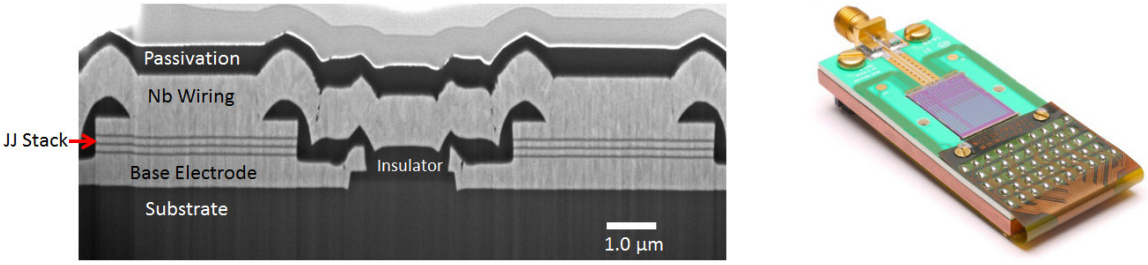

Figure 2. (Left) SEM image of a NIST 10 V PJVS circuit in cross section along propagation direction of the CPW center conductor. Two separate triple-JJ stacks can be seen. (Right) photograph of crypopackage developed for the NIST 10 V PJVS circuit. The chip size is 12 mm × 17 mm. Images courtesy of NIST Boulder precision imaging facility (SEM) and Dan Schmidt (cryopackage).

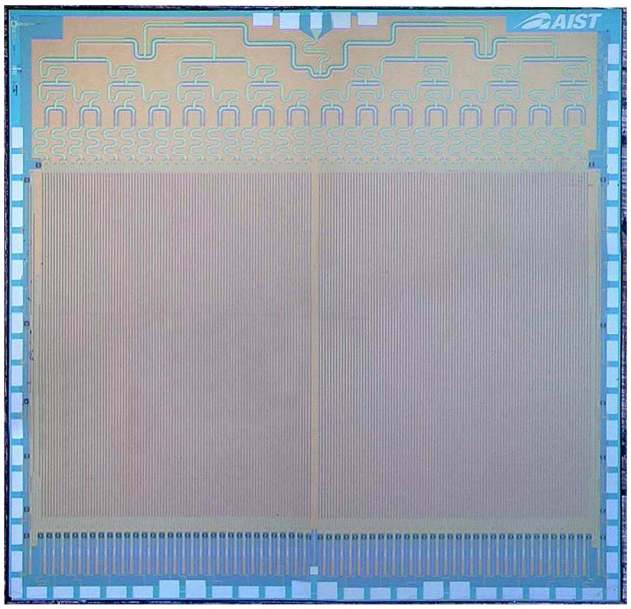

Figure 3. Photograph of 17 V NMIJ/AIST PJVS circuit including 524 288 NbN/TiN/NbN JJs. The chip size is 15.28 mm × 14.70 mm. Image courtesy of Hirotake Yamamori [31, 32].

Operation of a 17 V or 20 V PJVS circuit requires bias electronics designed with twice the output voltage compliance compared to 10 V circuits. The main secondary standards that are typically calibrated are the Zener dc references, which are calibrated at 10 V [36, 37]. So, a Josephson standard with an output voltage greater than 10 V [30, 32] has limited application for dc voltage calibrations.

Two other laboratories have developed PJVS circuits that have demonstrated lower voltages with alternative fabrication. The National Institute of Metrological Research (INRIM) in Italy, in collaboration with PTB, has developed a 1 V PJVS circuit based on superconducting-normal-insulating-superconducting (SNIS) junctions [38]. The Institute of Electronic Measurements (KVARZ) in collaboration with the Institute for Physics of Microstructure from the Russian Academy of Science was the first laboratory to successfully implement a voltage standard made of a high-temperature superconductor (HTS). The KVARZ HTS circuit has 161 JJs made of grain boundaries between two $YBa_2Cu_3O_7$ layers [39, 40]. The output voltage of this HTS-based circuit reaches about 25 mV and has the main advantage that it can operate at 77 K (i.e. liquid nitrogen instead of liquid helium temperatures).

A summary of the different types of PJVS circuits currently being fabricated and their main characteristics are presented in table 1.

The initial motivation behind the PJVS was to develop a quantum-accurate rms source [41], based on the calculated voltage levels of a stepwise-approximated waveform. Unfortunately, the ~1 µs switching duration (transients between steps) of the bias electronics developed in the mid 1990s limited the relative accuracy to 1 part in 10^5 at 1 kHz. Newer, faster electronics reduced the switching time and duration of the transients by more than two orders of magnitude, but realization of an accurate rms waveform synthesis with PJVS circuits was prevented by intrinsic systematic errors associated with the transients (see next section). However, development of measurement methods that eliminate the transients, namely those that exploit only the quantum-accurate portion of the steps in the PJVS stepwise waveforms, have opened numerous applications in ac voltage metrology for frequencies up to a few kilohertz. With programmable dc voltage and ac waveform capabilities, PJVS systems now largely surpass CJVS systems in both performance (i.e. intrinsic stability) and range of applications (see section 4). NMIJ/AIST, NIST, and Supracon, have successfully operated PJVS circuits on liquid-helium-free dry cryocoolers [42–44]. Fully automated, liquid-cryogen-free PJVS systems are available from NIST through the NIST standard reference instrument program[3] and from Supracon[4]. As turn-key systems, these cryocooled PJVS systems do not require an expert operator or cryogenic handling skills to be successfully and reliably operated. The ease of use of these systems extends the range of dissemination of PJVS from primarily NMIs to a larger number of calibration laboratories.

2.2. *Josephson arbitrary waveform synthesizer*

A JAWS system generates accurate output voltages by controlling the timing, presence, and polarity of the quantized pulses created by the JJs [45]. Like the PJVS system, the JAWS circuit requires long homogeneous arrays of JJs to generate useful voltages. Unlike the PJVS approach, in this case the JJ array is biased by a pulse generator so that during each clock

[3] NIST standard reference instruments: www.nist.gov/sri/standard-reference-instruments/sri-6000-series-programmable-josephson-voltage-standard-pjvs.
[4] Supracon AG: www.supracon.com/en/standards.html.

Table 1. Summary of PJVS circuits currently in fabrication. The circuits (columns) are sorted by bias frequency.

	NMIJ/ AIST [32]	NIST [24]	PTB/Supracon [29]	PTB [30]	INRIM/PTB [38]	KVARZ [40]
Voltage	17.3 V	10 V	10 V	20 V	1.19 V	25 mV
# of JJs	524 288	265 116	69 632	139 264	8 192	161
Bias Frequency	16 GHz	18.3 GHz	70 GHz	70 GHz	70 GHz	75 GHz
Junction Material	SNS NbN/ TiN_x/NbN	SNS $Nb/Nb_xSi_{1-x}/Nb$	SNS $Nb/Nb_xSi_{1-x}/Nb$	SNS $Nb/Nb_xSi_{1-x}/Nb$	SNIS $Nb/Al\text{-}AlO_x/Nb$	HTS grain boundary $YBa_2Cu_3O_7$ bicrystal
Temperature	<11 K	<5 K	<5 K	<5 K	<5 K	<77 K
# of JJs/Stack	2	3	1	2	1	—
# of JJs in LSB	128	6	1	2	—	—
LSB resolution	4.235 mV	227 μV	145 μV	270 μV	—	—

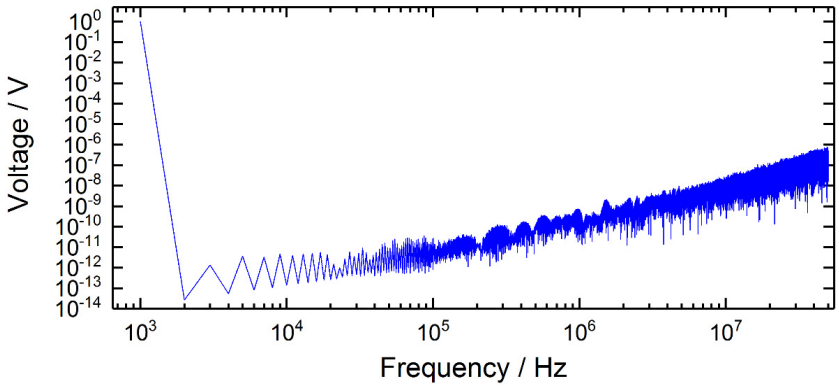

Figure 4. Calculated spectrum from dc to 50 MHz of a 1 kHz sine wave with rms magnitude of 1 V, based on 12 810 JJs and a clock rate of 14.4×10^9 pulses s^{-1}.

cycle, each JJ in the array generates either a positive pulse, a negative pulse, or no pulse. A repeating sequence of JJ voltage pulses has a voltage spectrum with a calculable, quantum-accurate magnitude and phase. The pulse sequence is typically determined using a delta-sigma modulation algorithm [46, 47]. In practice, a pure, 1 kHz ac voltage waveform (figure 4) can be created with a calculable spurious-free dynamic range (SFDR) greater than 200 dBc for frequencies up to 100 kHz [14] due to the large oversampling ratio between the clock rate (typically 14.4×10^9 pulses s^{-1}) and the frequency of the desired waveform (typically in the audio range).

As applied to JAWS circuits, the idea behind the sigma-delta algorithm is to step through the desired waveform as a function of time at the pulse rate and decide at each step (sampling period) whether the agreement between the desired waveform and the programmed waveform is better with a positive pulse, negative pulse, or no pulse. The decision is made using the output of a feedback loop whose input is the difference between the desired waveform and the pulse pattern at that time step, that is, the 'delta' in the algorithm name. The structure of the feedback loop can be more sophisticated with multiple loops but typically involves the summation of past errors, that is, the 'sigma' in the algorithm name [46, 47]. Typically, feedback loops used to calculate JAWS patterns for output voltages at frequencies <1 MHz contain two stages of integration and a low-pass filter. The net effect of this filter and algorithm is to move the digitization noise caused by the fast pulses away from the frequencies of interest (in this case, to >10 MHz), leaving a pure tone with a small background (see figure 4). After the entire pulse pattern is generated, the magnitude and phase of all frequency components are determined from a Fourier transform of the pulse pattern. Typically, both the pulse pattern and the calculated value of the relevant frequency components are stored for later use.

Two significant differences between other typical uses of the sigma-delta algorithm and how it is used in JAWS systems are: the need for high pulse density, and the use of pre-generated patterns. The maximum output voltage of the JAWS system is proportional to the maximum pulse density, which is typically taken to be between 90% and 95% (with 100% corresponding to a pulse at every clock cycle). Operation at high density reduces the stability of the delta-sigma feedback loop and can also result in excess digitization noise. In general, a pulse density above 50% would be considered 'overloaded' by the standard definition for a second-order algorithm [46, 47]. However, standard delta-sigma algorithms are often intended to be run in real time and accept or generate arbitrary waveforms as part of an analog-to-digital converter (ADC) or digital-to-analog converter (DAC), respectively. Because the JAWS waveforms are typically pre-generated, the delta-sigma algorithm settings can be tuned for a given output voltage, making the overload condition less important. This must be confirmed by checking that the frequency content of the pattern after generation produces no distortions.

The JAWS systems developed by both NIST and PTB use the same basic type of JJs as they use in their PJVS systems (described above), though the JJ properties are optimized for operation at around 20 GHz [23, 48]. The maximum output voltage and the number of JJs used in the JAWS systems is smaller than in the PJVS systems. PTB has recently created

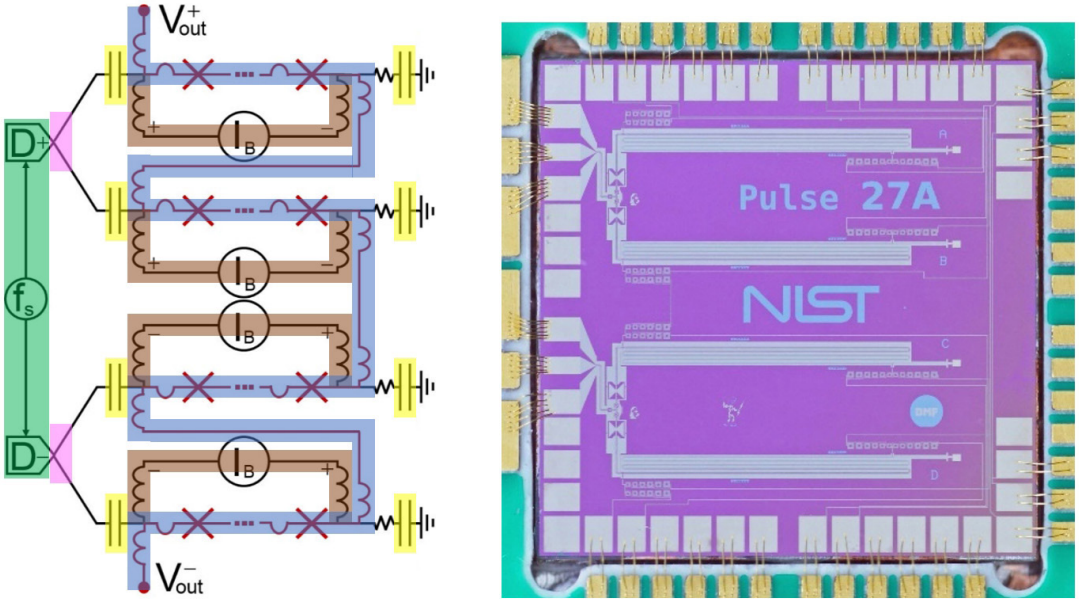

Figure 5. (Left) NIST JAWS circuit diagram and (right) photograph of a cryopackaged JAWS chip. The circuit can generate an output voltage of 1 V rms. The circuit includes two pulse generator channels (green, labeled 'D+' and 'D−'), a single layer of Wilkinson dividers (pink), inside-outside dc blocks (yellow), and JJ arrays (red 'X's). The JJ arrays are connected in series through inductive taps, as is one floating low-frequency current compensation per JJ array (brown, 'I_B'). The JAWS chip size is 10 mm × 10 mm.

waveforms with an rms output voltage of 1 V by summing the signals from eight JJ arrays operated on four separate cryopackages with a combined total of 63 000 JJs [12, 49]. NIST has recently summed two cryopackages with a total of 102 480 JJs to create waveforms with an rms output voltage of 2 V [13]. Many of the circuits fabricated by NIST [50–52] and PTB [53, 54] are used by other NMIs around the world.

In comparison to PJVS circuits, the smaller output voltage and number of junctions used in JAWS systems are directly related to the added complexity of the microwave pulse bias. Instead of a single-frequency bias, the JAWS pulse-pattern bias typically contains significant power at frequencies from 1 GHz to >30 GHz [14]. Therefore, the JAWS system is even more sensitive to the non-ideal behavior (e.g. non-linear response) of the circuit elements and the quality of the high-speed pulse bias source and amplifiers. To combat this sensitivity, JAWS circuits have adapted many of the elements developed for PJVS circuits, as shown in figure 5, and have also added many parameters and pulse generation methods to optimize the pulse bias [14, 55–62].

Like PJVS systems, JAWS circuits use JJs embedded in tapered CPW waveguides, and special emphasis is placed in the fabrication process on uniformity of electrical properties of the JJs [26]. These design and process features compensate for loss in the CPWs, so that the optimal input current pulse is similar for JJs at the beginning and end of each array. JAWS circuits use the same low-pass superconducting inductive taps as used in PJVS circuits to extract the output voltage across each JJ array [63]; the inductance prevents the taps from disturbing the high-frequency bias, while also having minimal effect at low frequencies. Finally, both the PJVS and JAWS systems use similar, though not always identical, on-chip resistive structures for microwave termination of the JJ arrays to avoid unwanted reflection.

Current PTB [12, 49] and early NIST JAWS circuit designs [64, 65] did not use explicit on-chip microwave power distribution elements (figure 6); instead, each JJ array was connected to the pulse generator through separate high-frequency, semi-rigid cables, connectors, and room temperature components. This direct connection was necessary to maximize the input bandwidth for the pulse waveform bias and minimize reflections in the pulse transmission path. This direct connection means that each JJ array was biased by a separate channel of the pulse generator. This approach had the advantage that the bias settings of each channel could be optimized to match the properties of each JJ array, but had the disadvantages that pulse generator channels are expensive. Every microwave cable also increases system complexity and heat dissipation at cryogenic temperatures.

Recent NIST JAWS circuits have adopted the on-chip power division approach used in PJVS and CJVS circuits by adding on-chip Wilkinson dividers, so that each pulse generator channel and microwave line can bias multiple JJ arrays [13, 14]. This drastically reduces system expense and complexity but also places more stringent constraints on the uniformity across the entire chip for both the frequency response of the on-chip microwave elements and the electrical properties of the JJs. That is, by biasing multiple JAWS arrays with a common pulse generator channel, one cannot independently optimize the pulse bias to each array. The removal of optimization parameters also typically reduces the range of bias parameters over which the system is 'quantum locked,' where one JJ output pulse is generated for every input pulse (see section 3.1 for details). This reduction in QLR makes the system

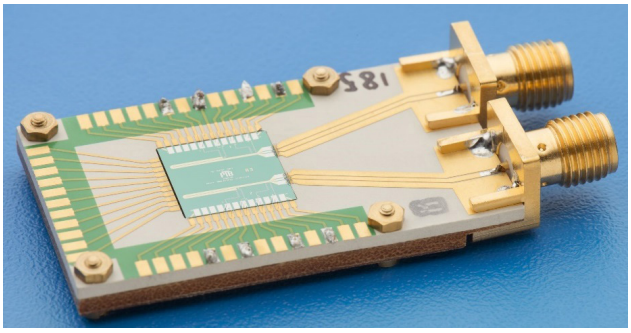

Figure 6. Photograph of JAWS circuit with two arrays of 6000 JJs fabricated by PTB. The chip size is 10 mm × 10 mm. Four sample holders and eight arrays are combined in series to reach 1 V rms (see [12] for details). Image courtesy of Johannes Kohlmann and Oliver Kieler.

more difficult to operate correctly and can affect stability. NIST's recent use of a finite-impulse-response (FIR) filter on the pulse generator outputs allows an improvement in pulse shape uniformity, which partially compensates for the added circuit components and circuit complexity [14, 66].

The use of Wilkinson dividers on the NIST PJVS and JAWS circuits requires the implementation of an additional passive on-chip microwave component: an inside-outside dc block between each JJ array input and Wilkinson divider outputs. This takes the form of capacitive breaks on the grounds and inner conductor of the CPW. This low-frequency isolation of the individual JJ arrays from the pulse generator is required so that the JJ arrays can be summed in series to generate larger, quantum-accurate voltages. The PTB JAWS system and earlier NIST JAWS systems use room temperature inside-outside dc blocks and maintain that isolation from room temperature to each JJ array.

The typical room-temperature equipment used by a JAWS system consists of pulse generators, broadband microwave amplifiers, and low-frequency, isolated current sources [58–61]. The generator's pulse repetition rate f (clock) limits the maximum output voltage $V = M \times f \times h/2e$ for M JJs, though typically other circuit components and the JJ properties also limit the maximum repetition rate. The generator's memory size, which determines the maximum duration of the synthesized waveform, places a lower bound on the output voltage frequency. In some cases, the output amplitude of a pulse generator channel is sufficient to bias a JJ array. However, in other cases, especially when dividers are used to bias multiple arrays, the pulses require additional amplification. The amplifier must meet stringent requirements of large output current, wide bandwidth, and small gain ripple. This is particularly true when driving arrays through Wilkinson dividers; at least 3 dB more power is required for each layer of Wilkinson dividers.

Finally, achieving the highest output voltage typically requires biasing each JJ array by a low-frequency, isolated, current source with the same shape as the desired JAWS output voltage waveform, often called a 'compensation' current. This requirement is a side effect of the need for inner–outer dc blocks to isolate the JJ arrays from the pulse generators in order to connect multiple arrays in series without common mode signals. The dc blocks are high-pass filters that shift the offset of each pulse based on the recent pulse-density history. This changing offset narrows the bias range over which the JJ arrays remain quantum-locked and the JAWS circuit produces accurate voltage waveforms. The current source 'compensates' for the shift by reintroducing the components of the spectrum removed by the filter. However, the compensation current is also a source of systematic error [62, 67, 68], as described below in section 3.2.2.

A separate solution to the presence of a high-pass filter is to change the shape of each pulse by removing the low-frequency content [61, 62, 66]. This is often called a 'zero-compensation' method. In the simplest version, a half-pulse of opposite sign is applied both before and after the conventional pulse. The spectrum of this 'pulse-like' object has very little power at the frequencies affected by the high-pass filter (i.e. inner–outer dc block), and therefore the filter has minimal effect on the pulse shape. After optimization, the non-linearity of the JJ response to the pulse-like object results in a single voltage pulse. Using this zero-compensation pulse-bias method both reduces the complexity of the electronics and removes sources of error in the output voltage. The main disadvantage of the zero-compensation method is that it reduces the maximum output voltage [66]. Each pulse-like group is spread over a longer time interval, thus reducing the maximum pulse repetition rate and the output voltage. In practice, there is usually a trade-off (that depends on synthesis frequency) between the need for higher voltage or improved signal-to-noise ratio and the need to remove frequency-dependent sources of error. Larger synthesized amplitudes at lower frequencies are typically synthesized with compensated biases, whereas at higher frequencies (>100 kHz) where systematic errors from compensation become significant, zero-compensated bias methods are used to produce lower-amplitude signals. The zero-compensation waveforms can also be directly compared to compensated waveforms as a function of frequency at lower voltages to better understand and characterize the systematic errors present in the higher-voltage compensated waveforms.

Unlike the CJVS and PJVS systems, JAWS systems have only recently begun to make the transition from being research tools towards becoming disseminated standards. This change is motivated by having reached an rms output voltage of 1 V, where the JAWS systems can begin to play a larger role in thermal convertor calibrations. An automated, liquid-cryogen-free JAWS system is now available from NIST through the NIST standard reference instrument program[5].

Over the past 30 years there has also been progress in making digital circuits using single flux quanta (SFQ): using JJs as active logical elements, instead of transistors [69]. One application of these circuits is to create a JAWS system in which the JJ array and the room-temperature pulse generator are replaced by an array of superconducting quantum interference devices (SQUIDs) biased by on-chip logic [70, 71]. To date, these systems have only found use in applications involving very small voltages [72, 73].

[5] NIST standard reference instruments: www.nist.gov/sri/standard-reference-instruments/sri-6011-josephson-arbitrary-waveform-synthesizer.

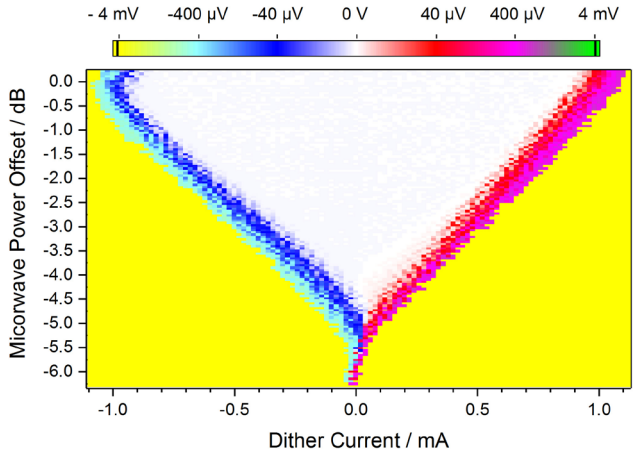

Figure 7. Two-dimensional quantum-locking range of a 10 V PJVS array with the subarrays biased such that exactly the same number of junctions are at +5 V and −5 V, producing a null voltage. The horizontal (x) axis is the dither current applied through all the subarrays, while the vertical (y) axis shows microwave power offset in dB relative to initial (optimum) power. The white area indicates the QLR where the output voltage remains constant. The measurement was performed on the 1 mV range of the digital nanovoltmeter.

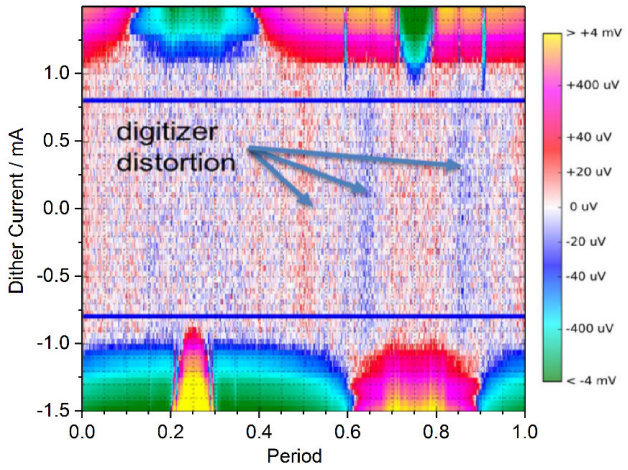

Figure 8. Graphical visualization of the quantum locking range of a JAWS system generating a 1 kHz waveform with an rms magnitude of 2 V (data from Flowers-Jacobs *et al* [13]). In the graph, the color at each point indicates the voltage residual of a sine-wave fit as a function of dither offset current (y axis) and waveform period (x axis). The data was digitized over 80 ms with a National Instruments PXI-5922 digitizer (range 10 V, input impedance 1 MΩ, sampling rate 1 MHz). The blue lines show the 1.6 mA quantum locking range of this waveform and system, that is, where the residuals are limited by digitizer distortion and do not depend on offset current over the entire waveform period. This visualization technique highlights the pulse sequences (e.g. at 0.25, 0.6, and 0.9 parts of a period) that limit the QLR.

3. Josephson quantum locking range and limitations

3.1. Quantum locking range

A Josephson voltage standard (JVS)[6] is operated within its its quantum locking range (QLR)[7] if every JJ produces a single voltage pulse ($n = \pm 1$) per input bias pulse. When biased on the QLR, the output voltage remains constant over a significant adjustable range around the step-centered bias parameters. A JVS can be in one of two states: either it is operated within a well-characterized QLR, and the output voltage generated by the JJ array is precisely known; or it does not have a QLR, and the output voltage is undefined. In the second case, the JVS cannot serve as a metrology reference. Measuring only the stability of the generated voltage over a long period of time, possibly with low uncertainty, is not a sufficient criterion to test the quantum accuracy of voltage standard; it simply tests the stability of the system biases and environment. If biased slightly outside its QLR the output voltage may remain stable (and probably very close to the ideal value) but will provide inaccurate voltages. For maximum confidence in output voltage accuracy, the JVS should be operated with the largest QLR achievable; ideally, the output should be confirmed during calibration measurements.

In principle, a JVS system should have a built-in procedure to self-check its QLR either manually or automatically. With the NIST PJVS system, the QLR is confirmed routinely with a commercial digital nanovoltmeter. To reach the maximum sensitivity of the nanovoltmeter, the subarrays are biased in series and with opposite sign to obtain zero net dc output voltage [18]. In this configuration, one or more parameters are dithered to determine the limits of the operating range (also known as the operating margin) and whether the voltage remains constant. The bias parameter most commonly tested is a dc offset current (also called dither current or trim current), which is applied to every subarray. In figure 7, two PJVS parameters, current offset and microwave power, have been varied from their initial (and optimal) bias setpoint while the output voltage, which was set to 5 V + (−5 V) = 0 V, is measured. The QLR is defined as the area or the range in which the voltage remains constant (white region at 0 V in figure 7). In this example, the microwave power can be reduced by more than 4 dB while still maintaining perfect voltage quantization, thus validating the operating parameters initially selected from the margin table of bias setpoints for all subarrays.

Because the JAWS waveform is periodic in time, the QLR is generally verified with a digitizer or a high-resolution oscilloscope. One method to determine the QLR is to add a low-frequency triangular sweep to the bias current compensation signal and measure the time-dependent distortion of the JAWS waveform. NIST has developed a graphical method (figure 8) for displaying QLR [13], where the ideal synthesized waveform is subtracted from the measured signal, and only the voltage residuals (distortion) are shown in a surface density plot. The vertical axis shows the dc offset current magnitude, while the horizontal axis represents one period of the JAWS signal. The central speckled band (white, light blue and light red) shows the QLR where the residuals are minimal. By monitoring the residual measurement while varying other bias parameter, the QLR area can be seen to shrink, thus determining the QLR for that parameter[8].

[6] 'JVS' refers to both PJVS and JAWS systems described in this manuscript.
[7] 'QLR' was previously referred to as 'flat spot' or 'margins range' in the literature.

[8] For a video example of the QLR display method see: www.nist.gov/pml/quantum-electromagnetics/superconductive-electronics/quantum-locking-ranges.

QLR verifications are primarily performed on JVS systems through automated software, where the voltage output leads are connected only to the nanovoltmeter (for PJVS) or digitizer (for JAWS). When a JVS is imbedded in a calibration or a more complex measurement circuit, then the initial QLR verification may not be easily accessible and cannot be performed automatically. In more complex measurements, additional factors such as the presence of current noise induced by undesired ground loops can reduce the QLR. In a worst-case scenario, these unaccounted perturbations could jeopardize the quantum accuracy of the measurement. One way to verify the quantum accuracy of the JVS reference without disturbing the measurement circuit is to repeat the measurement multiple times while successively applying an offset to one of the bias parameters, with the bias offset magnitude not exceeding the QLR. For example, the automated measurement sequence of a direct (dc) comparison between two PJVS systems can be programmed with three levels of offset current: 0 mA, +0.2 mA and −0.2 mA [10, 74]. During data analysis, if the voltage difference between the two PJVS systems is not correlated with the bias parameter change, then the quantum accuracy (or QLR over the tested range) is confirmed for the entire duration of the measurement. A similar verification approach is built into the NIST PJVS-Zener dc reference calibration measurement. Application of a similar verification method is strongly encouraged for all types of measurement involving any JVS, and especially with the implementation of a PJVS with a Kibble balance or Joule balance [75–80].

3.2. Limitations

Obtaining a well-defined QLR is the first validation test that should be completed before performing any calibration measurement with a JVS. However, other factors may still limit the accuracy of the JVS. For every JVS, the microwave or pulse-bias electronics must be locked to a reference frequency of high accuracy and traceable to the SI. As discussed in section 2, a JVS is a direct frequency-to-voltage converter. This means that the relative uncertainty in the frequency reference will be transferred with the same magnitude to the voltage uncertainty. Today, compact, commercially-available frequency standards can routinely achieve an absolute frequency accuracy better than one part in 10^{11}. Frequency standards can easily be made traceable to the SI anywhere on Earth with the use of a global positioning system disciplined oscillator [81].

The second limitation, also common to all JVSs, is the potential for the JJs to source current when the output of the JVS circuit is connected to a low-impedance load. Any current flowing in the voltage output leads will generate a voltage error due to the finite resistance of the wires. Driving excessive current out of the JVS device may also exceed the operating range of the JJs, such that the resulting loss of quantization will destroy the accuracy of the JVS voltage.

3.2.1. PJVS limitations. When a PJVS is operated to generate dc voltages, the two main error contributors are the thermal electromotive forces (EMF) and voltages generated from leakage currents. These errors are due to the finite resistance of the voltage output leads and the temperature gradient between the PJVS circuit at ~4 K and instruments connected at room temperature. Thermal EMF errors can easily be eliminated by performing polarity reversal measurements. Leakage current errors can be limited by properly engineering the JVS bias electronics and by using a material with high isolation resistance for all leads connected to the PJVS circuit.

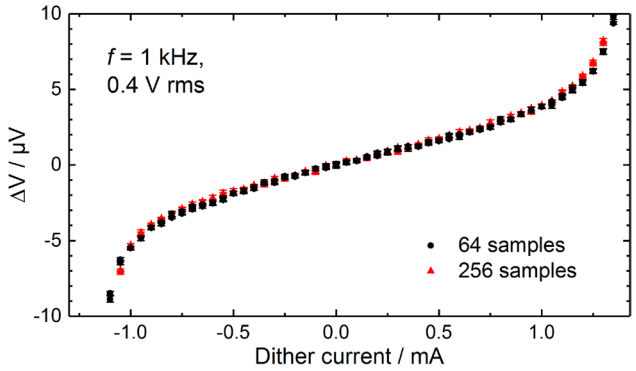

Figure 9. Relative change of rms voltage measured with a thermal transfer standard for a 0.4 V stepwise-approximated sine wave versus applied dither current. The voltage value at 0 mA is used as the reference for the voltage difference ΔV. The slope observed within the ±0.7 mA dither range is due to transients present in the waveform; the QLR of the PJVS array when generating dc voltages is ±0.7 mA.

Direct synthesis of PJVS ac waveforms is undesirable for rms calibration of devices under test (DUT) such as ac voltmeters, TVCs and thermal transfer standards (TTSs). The finite rise time of the current bias-electronics and the stepwise nature of the waveforms introduce multiple non-negligible systematic errors. Development of faster switching bias electronics [82] or techniques to drive low impedances [83, 84] do not eliminate this inherent problem. The rms value of a PJVS step-wise approximated output waveform is never fundamentally accurate; a small change in one of the PJVS bias signals, such as the bias current to one subarray or the applied microwave power, has an influence on the rms output voltage. For a review of this error mechanism, see Burroughs *et al* [85, 86]. Many measurements in the literature have been subject to such transient problems [83, 84, 87–98]. As an example, figure 9 shows the absence of accurate voltage over the range we expect to observe a QLR (data from Burroughs *et al* [85]). The plot shows the effect of current bias offset on the rms voltage measured by a thermal transfer standard operated with a high input impedance. Due to transient effects, the magnitude of the slope varies almost linearly with frequency [85]. PJVS stepwise-approximated waveforms contain large numbers of harmonics [89], with the magnitude of the harmonics (including the fundamental) affected by the transients [99]. The use of a two-level PJVS waveform is one way to slightly minimize the effect of transients on the fundamental [100], but it has the undesirable consequence of generating a large quantity of large-amplitude digitization harmonics. The use of two-level PJVS waveforms has been implemented for fast reverse dc measurements [101, 102] and was suggested for impedance ratio measurements based on two PJVS systems [90, 91, 93, 95–98].

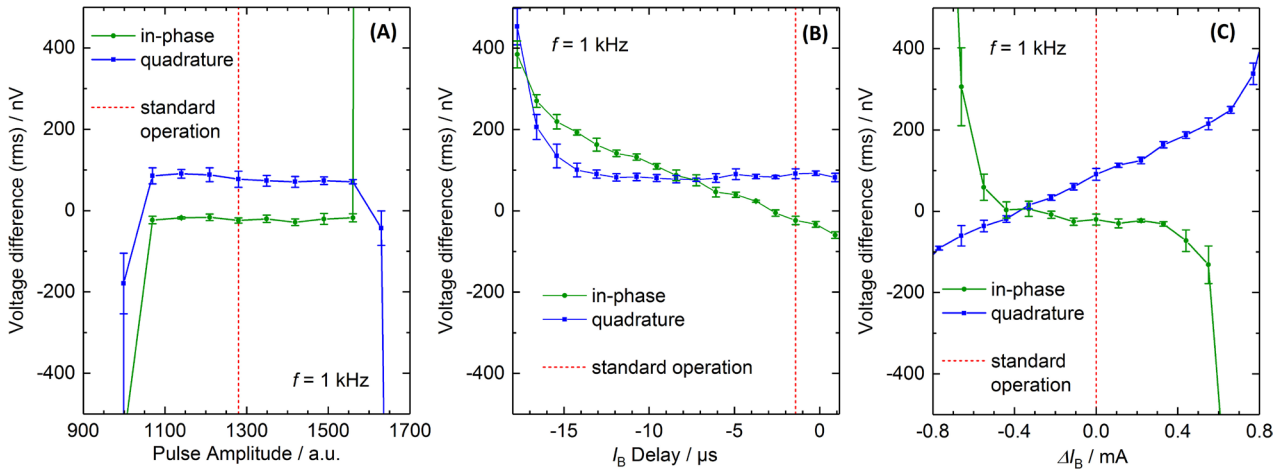

Figure 10. In-phase (green) and quadrature (blue) magnitudes of the residual difference between two NIST JAWS systems, each generating a 1 kHz output with an rms magnitude of 1 V, versus different bias parameters. The standard operating point (vertical red dotted line) is the bias setting that maximizes the QLR for dc current offset. (A) The residual magnitude is independent of the pulse magnitude (within the QLR from about 1100 to 1550) but in depends strongly on (B) compensation phase and (C) compensation magnitude. The phase is expressed in terms of the time delay of the compensation relative to the pulse generator output, while the compensation magnitude is expressed as a change ΔI_B from the standard operating point of about 10 mA.

As shown in figure 9, tuning just one of the bias signals will always modify the transients in some fashion and results in a change in rms voltage. If the rms value of the transients matches exactly the rms value of the PJVS waveform, then the rms output is independent of the waveform frequency selected. This special operating bias point (the intersection of curves at different waveform frequencies) was first determined experimentally in TTSs and TVCs [83, 85, 103] and later described in detail by Burroughs *et al* [104]. However, the independent tuning method (without relying on a TVC standard) is rather fastidious, and the accuracy of the method remains affected by any external perturbations including current noise, stability of the bias electronics and changes in microwave power due to changes in the liquid helium level in the dewar [104]. Due to transient-related errors and the resulting lack of quantum accuracy in rms amplitude for stepwise-synthesized waveforms, most rms measurements with PJVS systems have been abandoned. Sampling or differential-sampling methods, which avoid the effects of the transients, are recommended for performing ac voltage calibrations with stepwise PJVS waveforms (see section 4).

3.2.2. JAWS limitations. The JAWS system shares some of the same basic limitations as the PJVS, but the dominant source of systematic errors changes as the waveform frequency increases above about 10 kHz. Thermal EMFs play a similar role as in the PJVS system. However, current flowing in the circuit can have a much more pervasive effect as a function of frequency. Specifically, systematic errors will arise from both the compensation current through the JJ arrays mentioned earlier [62, 67, 68] and the current flowing in the output leads between the JJ arrays and the DUT [51, 67, 105–107]. This second source of error is typically called the 'voltage lead' error or correction.

Thermal EMFs will affect the JAWS output voltage and cause offsets in rms or power measurements. This will particularly affect small amplitude measurements, although a stable thermal EMF can be removed by performing a polarity reversal measurement as is done with the PJVS. On the other hand, AC measurements, which separate lower-frequency noise from higher-frequency signals of interest will not be affected by thermal EMF. Nevertheless, a system design that minimizes the thermal EMF is still worthwhile because it simplifies data analysis and improves system stability.

As mentioned at the end of section 2.2, the compensation current applied using isolated current sources is a source of systematic error [61, 62, 67, 68] but can be avoided with use of zero-compensation waveforms if the reduction in output voltage is acceptable. Because the JJ array is inductive, compensation currents create an error voltage with frequency-dependent amplitude that is approximately 90° out of phase with the desired output voltage. In a typical NIST JAWS system generating an rms output of 1 V at 1 kHz with a total inductance of about 50 nH and compensation current amplitude of about 10 mA, the resulting error voltage has an rms magnitude of about 3 µV. The magnitude of this error voltage increases linearly with frequency and compensation amplitude.

The impact of this systematic error can be calculated by effectively measuring the JJ array inductance, the magnitude of the compensation current and the phase of the compensation current relative to the synthesized waveform from the JJ array. Figure 10 shows the dependence of output voltage on compensation current. As in the earlier PJVS example (figure 7), we obtain the maximum voltage resolution from a null measurement resulting from the sum of two waveforms with the same, 1 V rms magnitude and opposite phase. The residual voltage difference is measured by a digitizer and expressed in figure 10 in terms of the in-phase and quadrature components. A bias parameter for one of the waveforms is then slightly detuned from those for 'standard operation' where the QLR in response to a dc current offset is maximized.

Another possible source of error is a low-frequency current from the pulse generator. Although this current should be removed by the dc blocks, an error voltage with a magnitude and phase that depends on the details of the system will occur at higher output waveform frequencies [68, 108]. The magnitude of this error can be determined by changing the amplitude of the bias from the pulse generator. In figure 10(A) we observe the desired behavior, where the residual voltage is not dependent on detuning of the pulse magnitude while the JJs are in the QLR.

In figures 10(B) and (C) we detune the compensation phase and magnitude, respectively, and observe significant changes in the residual voltage even while the system is quantum locked. These changes are consistent with the above model of an error voltage generated by compensation current passing through the JJ arrays. Because the error voltage is approximately in quadrature with the generated voltage, small changes in phase will linearly affect the in-phase residual voltage while having minimal effect on the quadrature voltage. Similarly, small changes in magnitude will linearly affect both the quadrature and in-phase residual voltages, but the scale of the effect will be significantly smaller for the in-phase residual voltage.

A more fundamental source of error is current flowing in the output leads [51, 67, 105, 106]. This current can have two sources: leakage paths and the impedance of both the voltage output leads and the device under test. The first case is identical to that of the PJVS, except that stray capacitances will also result in leakage currents with frequency-dependent magnitudes. In the second case, the fact that the JAWS is an ac voltage source causes more significant errors due to the impedance of the connecting leads and the inputs of the DUTs. The PJVS system operating at dc typically uses precision dc voltmeters that have a large input resistance >1 GΩ and leads with resistance $< 1\Omega$. Inductances and capacitances have no effect, so the output leads and DUT cause a simple voltage division at the DUT and an error of <1 nV at 1 V dc. On the other hand, ac instruments typically have input resistances <10 MΩ, and the input shunt capacitances >10 pF cannot be neglected. The combination of the DUT input impedance, on-chip inductance of the JJ arrays and inductive filters, and the cable inductance and capacitance typically results in a resonance between 10 MHz and 100 MHz [109]. The tail of this resonance has a significant effect on ac measurements above 100 kHz that is proportional to the frequency squared [51, 67, 105–107].

The effect of the output leads is exacerbated by the long leads needed to reach cryogenic temperatures. If the JJ arrays are cooled with liquid helium, then the output leads are typically about 1.5 m in length, whereas cryogen-free systems typically have leads that are longer than 0.5 m. Shorter leads are possible and would reduce the error voltage [53], but can result in a significant heat load on the cold stage. An alternative approach is to attempt to flatten the frequency response of the leads by adding additional impedance [108, 110].

Figure 10(C) also directly highlights the importance of accounting for sources of systematic error and detuning bias parameters when making comparisons between systems. In this case, we see that reducing the compensation magnitude by about 0.4 mA gives a measured difference of approximately zero between the two systems. Further averaging and fine-tuning of the compensation magnitude and phase could allow the systems to agree with a type A uncertainty limited only by the stability of the system. However, this would not represent the true agreement; in practice, the effect of the compensation current and all the other bias parameters must be measured and accounted for, either in the reported value or in the type B uncertainty.

4. Present applications of PJVS and JAWS systems

4.1. dc applications of JVS

In principle, dc voltage calibrations can be performed by either PJVS or JAWS systems. If the voltage output of a JAWS system reaches 10 V in the future, one might expect that JAWS systems will supplant PJVS systems for dc applications. However, it will be difficult to decrease the magnitude of JAWS leakage currents to that of PJVS systems and difficult to reduce the instrument cost of the necessary multichannel pulse generator to match that of a single microwave source. Until now, PJVS circuits show the largest practical output voltages, and dc voltage calibrations that require programmable voltages are presently performed almost exclusively with PJVS systems.

The main dc application for PJVS systems is the direct calibration of secondary voltage standards [111]. With the near total elimination of the use of chemical cells (Weston cells) from NMI laboratory benches, the secondary standard for dissemination of the unit volt is the temperature-controlled Zener dc reference at 10 V [36, 37]. Although these devices have been well engineered to minimize sensitivity to environmental conditions and their inherent drift has been reduced to a few μV/V per year [112], their output voltage remains dependent on variations in temperature, atmospheric pressure and humidity. To build a history and establish confidence in its predicted value and uncertainty, a Zener dc reference must be regularly calibrated [113]. The principal advantage of a PJVS system over a CJVS system is that its output voltage can be adjusted to perfectly match the Zener dc reference voltage with use of the bridge measurement configuration. A digital nanovoltmeter can then be used to measure very small residual voltages (typically <1 μV, corresponding to the magnitude of thermal EMFs in the circuit). With no voltage step jumps, unlike CJVS, the calibration duration may also be shorter. Another application of PJVS systems is calibration of gain and linearity of voltmeters [114, 115] and ADCs, which requires the rapid programmability of PJVS systems.

With a greater immunity to external noise than CJVS systems, PJVS systems can also be implemented in applications such as the direct calibration of the dc range of commercial calibrators and DACs [116]. Another application is the calibration of voltage ratios; for instance, DVM ratio calibrations

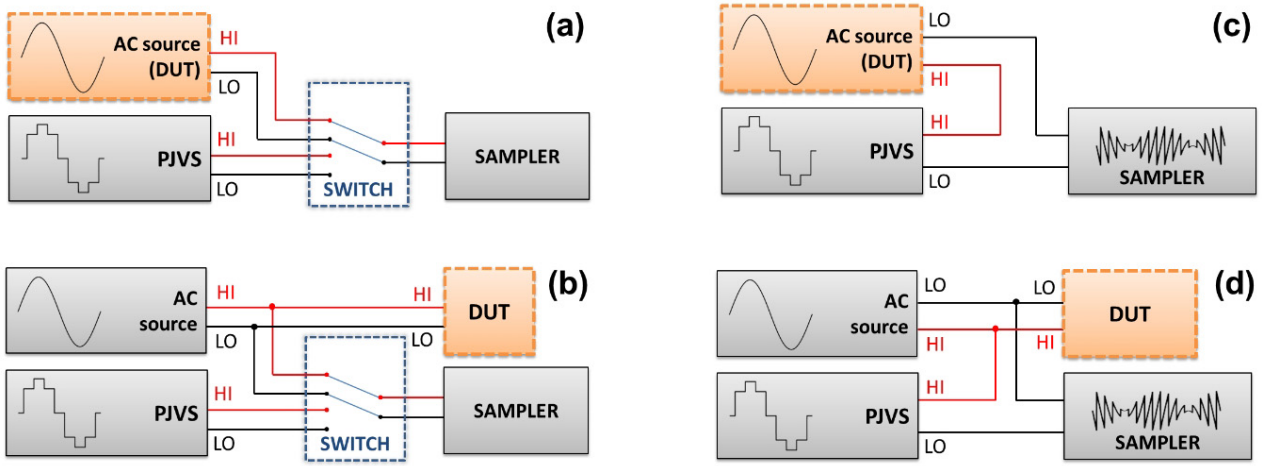

Figure 11. Diagram of various sampling methods: (a) and (b) sampling and switching and (c) and (d) differential sampling. The DUT can be an ac source, as shown in (a) and (c), or the source output can be connected to a DUT, as shown in (b) and (d). Synchronization signals to the various instruments are not shown in these diagrams for simplicity.

are required for applications such as measuring load cells used in mass metrology [117]. NIST is currently working to extend the dual-voltage output option on a single PJVS system from the 2 V circuit [118] to the 10 V circuit, eliminating the need for a Zener dc reference for the ratio calibration.

The dc calibration of nanovoltmeters cannot be performed with a single PJVS system, because the voltage resolution is limited by its LSB (see table 1) or, at best, would be defined by the voltage of a single JJ (typically many microvolts). To generate voltages with amplitude less than a few hundred microvolts, one method has been to use two independent PJVS standards in a differential configuration [119–122]. The same differential configuration is obtained when performing a direct comparison of two PJVS standards. By slightly detuning the microwave bias frequency of one PJVS circuit, the gain calibration of the nanovoltmeter can easily be measured [8, 10, 74, 123]. Other methods to generate low-amplitude dc voltages (and ac voltages with the same principle) involve reducing the pulse density with JAWS standards [124] or developing a PJVS circuit with dual microwave bias signals with independently tunable frequencies.

In addition, other metrology applications rely on the accuracy of PJVS systems. The electronic kilogram experiments with Kibble balances [75–79] and the Joule balance [80] were the first metrology applications of 1 V PJVS systems. Kibble and Joule balances will become a practical way to realize the unit of mass after the proposed SI redefinition [125]. Another example is the quantum metrology triangle, where electrical quantum-based measurements are expected to verify the consistency of three electrical quantum phenomena: the Josephson effect for voltage, the quantum Hall effect for resistance (QHR), and single electron tunneling for current [126, 127]. More recently, an elegant method to realize the unit ampere was proposed by coupling two electrical quantum standards (PJVS and QHR) with a cryogenic current comparator [128].

New research efforts are focused on extending the PJVS calibration range beyond 'core' voltage reference applications. Recent work presented the concept of dc current measurements with a calibrated current shunt and the measurement of dc resistance ratios with a commercial calibrator to supply the current [129]. This 'quantum calibrator' approach still requires an independent calibration of the current shunt or the reference resistances, and the overall accuracy of the measurement relies on the stability and performance of the commercial calibrator used as a current source.

4.2. AC application of JVS

4.2.1. PJVS stepwise approximated waveforms. The only accurate way to exploit a stepwise-approximated PJVS waveform for ac metrology is to implement a measurement method that avoids the transients. Only those portions of the PJVS waveform where the voltage is fully settled can be used as a voltage reference for ac signals. With this constraint, a logical measurement approach is to use sampling methods. Two types of sampling methods have been implemented with PJVS waveforms: sampling plus switching (or multiplexing) and differential sampling.

In either case, the goal of sampling is to transfer the accuracy of the PJVS reference waveform to a custom or commercial ac source. The output of the ac source can then be connected directly to a detector (e.g. ac voltmeter, TTS, TVC) as long as the source can provide the necessary loading current to drive the detector. In this case, the sampler and the PJVS, which acts as a sense input, should be placed as close as possible to the detector reference plane (figure 11). Both sampling methods require a stable ac source with high spectral purity. Undesired harmonics in the frequency bandwidth of the sampler could create aliasing effects on the fundamental of the waveform and potentially induce systematic error in the rms voltage reconstruction.

The 'sampling plus switching' PJVS method was first demonstrated by PTB for the electric power standard [130]. A slightly different version was implemented at METAS based on comparing the fundamental harmonic of ac source waveforms to the PJVS [99, 131, 132]. Switching methods rely on the measurement capabilities of the sampler over the full waveform amplitude range (peak-to-peak). To minimize

errors due to sampler non-linearity, the amplitude of the PJVS waveform is adjusted to match that of the ac source waveforms. Synchronization between the ac source, PJVS circuit, sampler and switching unit (multiplexer) is recommended to remove the transient contributions from the PJVS waveform and to facilitate rms amplitude reconstruction. However, the switching approach does not require phase alignment between the two waveforms. One factor to consider in the measurement uncertainty is the resistive divider effect between the resistance of the leads connecting the PJVS array to the sampler input terminal and the input impedance of the sampler. The magnitude of this effect is typically less when the multiplexer is connected to the ac source (assuming an ideal output source impedance) due to a shorter cable and hence lower resistance on the ac source path.

The concept of PJVS differential sampling with an ac source was first proposed by PTB [133] and was first demonstrated experimentally at NIST [134]. Further developments and applications of the differential sampling method followed at various NMIs [135–139], including the expansion of the rms waveform amplitude up to 7 V [140–142] and 10 V [143, 144]. With the differential sampling method, the sampler is used in a null-detector configuration, thus reducing errors due to the gain, non-linearity and input impedance of the sampler. To minimize the differential voltage measured by the sampler, the PJVS waveform shape, amplitude and phase are adjusted to match the ac source waveform. This can be achieved only if the three instruments (PJVS, ac source and sampler) are locked to a common frequency reference. Presence of phase jitter, produced by either the ac source or the sampler, will automatically translate to an apparent increase in voltage noise in the differential voltage measurement, an effect inherent to the differential sampling method. As a result, the rms output of the ac source is attributed with a larger type-A uncertainty and does not reflect the real amplitude stability of the source. The jitter effect can be observed with ac sources (ac voltage calibrators) phase-locked at the same frequency as the generated waveform. This inherent effect is only masked and hidden—not eliminated—by performing an average of the differential voltage signal over a large number of periods.

The results of the sampling method should be independent of the selected number of steps in the PJVS waveform. Adding more voltage steps per period (N) for the PJVS waveform has the benefit of reducing the differential voltage at the input of the sampler. This is a definite advantage if the amplitude of the ac source waveform is large and the input range of the sampler is limited [140]. However, increasing N reduces the duration of the well-defined voltage for each step of the waveform. Generally, shorter sampling duration (or aperture duration) increases the noise in the voltage measurement [120, 145]. The same reduction effect of the sampling window arises if the frequency of the waveform increases for a given value of N, because the transient duration remains the same. Typically, differential sampling methods are limited to waveform frequencies below a few kilohertz. Subsampling methods have been proposed to extend the frequency of the ac source while keeping the reference PJVS waveform frequency f below 1 kHz [146].

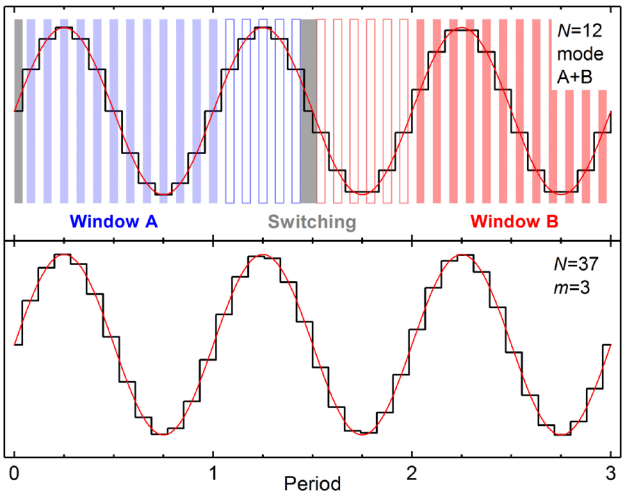

Figure 12. Example of two types of PJVS reference waveforms to track the ac source over multiple periods. (Top) alternating sampling windows (A) and (B) are shifted by $T/2N$ to cover the full range of the ac source period in the same measurement. (Bottom) the PJVS reference is adjusted to match the ac source over $m = 3$ periods.

Due to the presence of the transients, the sampling windows do not usually cover a full period $T = 1/f$ of the ac source signal. The rms amplitude calculation uses a sinusoidal model with an applied fit or fast Fourier transform, which may be inaccurate if the ac source has spurious harmonics [147]. One method to recover the full rms content is to combine two distinct measurements with shifted sampling windows A and B [148]. This principle can be applied to a single measurement by programming a PJVS reference that covers multiple periods of the waveform (figure 12, top). In this model, the sampling duration corresponds to 50% of the PJVS step duration, or $T/2N$. When the switching occurs between the PJVS reference A and PJVS reference B, no precision measurement can be performed (Gray zones containing PJVS transitions separated by $T/2N$ instead of T/N standard duration). Programming a PJVS waveform with multiple periods for each reference A and B, interleaved with the switching period, may improve the overall efficiency of the method. Compared to the two distinct measurements [148], a single measurement may more accurately track the short time stability of the source and may reduce overall uncertainty.

Another approach is to generate a PJVS reference waveform that tracks the ac source over m multiple periods (figure 12, bottom). In this case, either N or m is often chosen to be an odd number. Over m periods of the ac source, the sampling windows will cover the entire ac source waveform. One limitation of this method is that the frequency $f = (m/N) \times f_{\text{PJVS-Clk}}$ of the ac source waveform may not always have a fixed decimal value. To facilitate the removal of transients, $f_{\text{PJVS-Clk}}$ must be an integer sub-multiple k of the sampler digitizing frequency f_s (i.e. $f_{\text{PJVS-Clk}} = f_s/k$). This technique can also be used to match some ac source frequencies that cannot be commensurate with either $f_{\text{PJVS-Clk}}$ or f_s over a single period (for instance, at $f = 60$ Hz with $m = 3$, $N = 100$ and $f_s = 10$ MHz). Ultimately, for both methods shown in figure 12, the memory size of the PJVS bias electronics limits

the number of PJVS samples N and indirectly the number of periods that can be programmed.

Examples of applications in which PJVS sampling or differential sampling methods have been implemented include calibration of ac sources (called 'ac quantum voltmeter' by PTB and Supracon) [138, 140–144], electric power standards [130, 149], calibration of TTSs and TVCs up to ~1 kHz [131, 137, 141], and dynamic linearity measurement of ADCs [150].

4.2.2. JAWS applications. The main focus of the initial JAWS systems was the calibration of TTSs using single-frequency and DC waveforms [110, 151, 152]. A desire to expand the calibration range has pushed the development of higher output voltages [13], to the point where it is now possible to directly calibrate the high-impedance ranges of typical TTSs. Progress has also been made on using dividers to calibrate standards' higher voltage ranges [52, 153]. Further improvements in direct calibration will require accommodating lower input impedances, perhaps by using buffer or transconductance amplifiers [72, 153–155] similar to the one developed for implementation with a PJVS [83, 84]. Reaching higher frequencies will require improved methods for limiting the systematic errors from the output leads, as discussed earlier [51, 67, 105–107].

JAWS waveforms have been used to calibrate and characterize the non-linearity of electrical components using a variety of waveforms: dc offsets and single tones [124], two-tone waveforms in a general setting [156], and many tones as a key component in Johnson noise thermometry [157, 158]. Johnson noise thermometry extracts temperature by measuring the Johnson noise of a resistor and these systems have recently been used to measure the value of the Boltzmann constant [159–161]. JAWS waveforms are used to calibrate the entire measurement chain with μV/V precision at frequencies up to 1 MHz, directly enabling μK/K temperature measurements. In this context, the JAWS source is often called a quantum voltage noise source (QVNS) because a 'pseudo-random' JAWS waveform is used, that is, a comb in the frequency domain, with a magnitude approximately matched to the expected Johnson noise.

JAWS systems have also begun to be used as the dual voltage sources in both two-terminal [162] and four-terminal [163] automated impedance bridges. The advantage of JAWS sources is that they can generate ac voltages (with arbitrary relative magnitude and phase) on command so that a single bridge can compare any two impedances in an automated fashion. Typical high-precision bridges are manually operated and use transformers as dual sources which severely limits the type and value of the impedances that can be compared using any single transformer. This shift from transformers to JAWS systems has the potential for massively simplifying and automating ac impedance metrology.

Finally, as will be discussed in more detail in the next section, an important use of JAWS systems is for intercomparions with other JAWS [50, 164] and PJVS systems [49, 50, 165, 166]. While both JAWS and PJVS systems use JJ arrays, the bias circuitry is sufficiently different that such comparisons allow much to be learned about systematic errors. In particular, pure JAWS ac waveforms can enable measurements of systematic errors present in PJVS systems operated away from dc, and the effort taken to remove sources of error at dc in PJVS systems will help improve the performance of JAWS systems at dc.

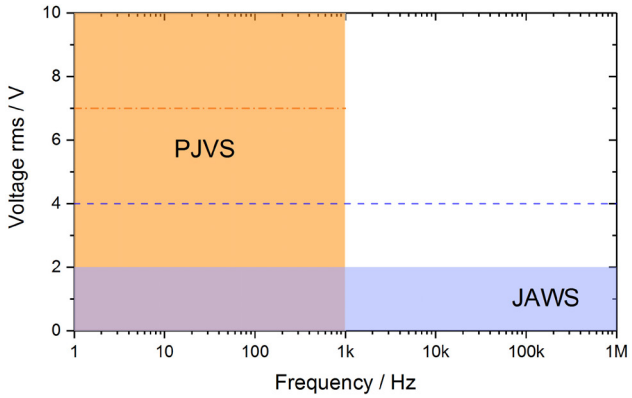

Figure 13. Voltage versus frequency diagram showing the application range of sampling methods for PJVS and JAWS. The blue dashed line shows the future extension enabled by ongoing research at NIST to develop JAWS circuits with 4 V rms amplitude. The red dash-dotted line represents the rms amplitude limit of 10 V PJVS circuits.

5. AC voltage metrology within the new SI

With the forthcoming redefinition of the SI, both PJVS and JAWS systems will become key components for the direct realization of the unit volt. This has implications not only for dc voltage metrology, but could also have a huge impact for the future dissemination of ac voltages. For more than three decades, dc voltage metrology has relied on quantum-accurate sources (CJVS and PJVS) to represent the unit volt ($K_{J\text{-}90}$) and to calibrate secondary voltage standards (Zener voltage references). Currently, ac voltage metrology is uniquely based on rms detectors (TVCs or TTSs) that typically require long calibration durations to 'fingerprint' each artifact's behavior as a function of both voltage and frequency. In principle, a switch from detector-based to source-based references can be applied to ac voltage metrology as well. Sampling or differential sampling methods are applicable to both PJVS waveforms (see section 4.2.1) and JAWS waveforms [164, 167], overlapping most of the frequency and voltage domain currently covered by TVCs and TTSs (figure 13). The accuracy of JAWS and PJVS reference waveforms must be transferred to low-noise and stable ac sources capable of driving low-impedance loads. Such ac sources would fulfill the role of secondary ac voltage standards in the same way Zener standards are used to disseminate dc voltages. To significantly impact dissemination of ac voltage, the amplitude stability of the ac source must be of the order of 1 part in 10^7, a value comparable to the performance of the best TVCs. Unfortunately, today's commercially available calibrators, with a short-term stability around 1 parts in 10^6, are not sufficient to perform this role. Additional requirements on the ac source include low harmonic distortion and

the ability to synchronize to an external time base to enable sampling methods. From an instrument design point of view, achieving sub μV/V stability and excellent spectral purity are not easily engineered. To reach these higher performance levels, the thermal stability of the electronic components inside the instrument plays a significant role, as does the DAC architecture.

When an ac source is used in direct combination with JVS standards, its absolute accuracy is not important. In this case, the key consideration is the source's short-term stability, so that the ac voltage can be accurately transferred from the JVS to the DUT (see figures 11(b) and (d) above). However, if the internal voltage reference of the ac source can be monitored and the ac transfer function calibrated at regular intervals with a JVS and a sampling method, such an ac source becomes a 'true' standalone secondary ac voltage standard. The accuracy of the ac amplitude is inferred from the measured dc reference and the calibration factors based on the amplitude, frequency and phase of the waveform generated. A source prototype based on this approach has been developed by Nissilä *et al* [168].

The successful dissemination and excellent performance of existing detector-based ac voltage metrology has not provided incentive for precision instrument manufacturers to develop ac sources with better accuracy and stability. Hopefully, the potential for improved ac metrology with readily-available, SI-realizable ac quantum standards will promote a paradigm shift in ac metrology and spur innovation in the instrument market, in term of both sources and samplers. This paradigm shift would take full advantage of the order of magnitude improvement in the stability and accuracy provided by the JVS standards.

An alternative approach to a new ac source is to develop methods for JAWS systems to directly drive low-impedance loads without compromising waveform accuracy. This approach would certainly not revolutionize the existing detector-based ac metrology but would offer a faster and intrinsic method to calibrate the ac–dc difference of TVCs. Because of the systematic errors due to transients, this approach cannot be successfully applied to PJVS waveforms (see section 3.2.1).

6. Comparison of JAWS and PJVS

The proposed redefinition of the SI also provides new incentive to reconsider the way traceability is currently implemented at NMIs. The dissemination of the unit volt within a nation is often traceable to a unique Josephson ('gold') standard. This 'legal' approach is inconsistent with the universality of the Josephson effect and its ability to realize the volt anywhere. The issue of traceability and equivalence of JVS systems was already raised two decades ago [2] as formulated in the following statement from Hamilton [169]:

> "Because of its realization of a quantum physics phenomenon, and the adoption of that phenomenon as the basis of the SI Volt Representation, a properly realized Josephson standard is correct by definition. The Josephson array device and the metrological system based on it constitute an intrinsic voltage standard. Comparisons between a Josephson standard and any other primary standard, including another Josephson standard, never lead to a new calibration value for the Josephson standard, but rather to a level of confidence that the Josephson standard itself is functioning correctly (no unaccounted-for errors exist). Periodic comparisons between the JVS and other primary standards are required to ensure proper operation".

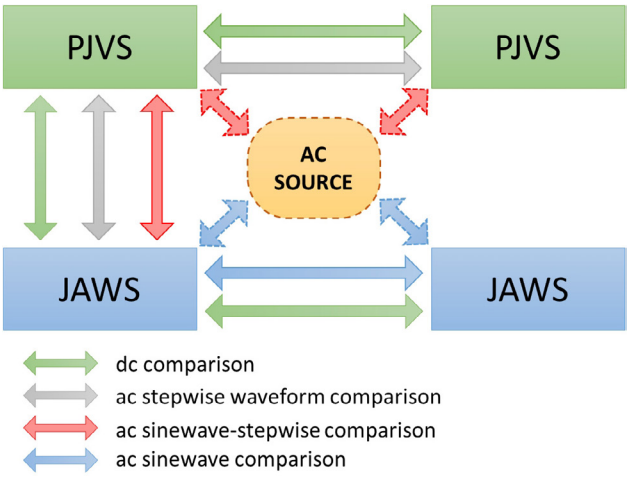

Figure 14. Schematic of direct and indirect comparison possibilities between two PJVS, two JAWS, or a JAWS and a PJVS voltage standards. The diagonal arrows with dashed outlines show indirect comparison links with an ac source as a transfer standard.

Even after the expected 2019 SI redefinition, when JVS systems will provide a direct realization of the SI unit volt and not merely a representation, this statement will continue to remain valid by replacing 'representation' with 'realization.' Determining the level of confidence in comparisons of JVS systems will become even more relevant in the presence of many disseminated 'nominally equivalent' Josephson systems that are all intrinsic standards. To verify the equivalence of two PJVS, two JAWS, or a JAWS and a PJVS, new comparison protocols must be implemented for both dc and ac voltages. As the schematic in figure 14 shows, some comparison possibilities use an ac source as the transfer standard (indirect comparison). The different types of comparison measurements can be grouped into four categories:

(1) dc to dc comparison
(2) ac stepwise to ac stepwise comparison
(3) ac sinewave to ac stepwise comparison (direct and indirect)
(4) ac sinewave to ac sinewave comparison (direct and indirect).

6.1. DC to dc comparisons

Presently, key comparisons of JVS systems for dc voltages follow a well-established BIPM protocol [170] designed to be implemented with the BIPM (CJVS) traveling standard [171]. Multiple direct comparisons between PJVS and CJVS systems [8, 9, 172–174], and between two PJVS systems

[10, 44, 74, 123, 130, 141] have been performed at NMIs and calibration laboratories. But, the comparison of dc voltages should also include JAWS systems [175]. The different microwave bias used by JAWS and PJVS systems means that performing a dc JAWS-to-PJVS comparison would provide an intrinsic verification of JAWS voltage accuracy without the influence of inductive errors that arise with ac waveforms. Such dc comparisons can also provide important information about the magnitude of the dc leakage current error within the measurement circuit and are an easy way to demonstrate the fundamental equivalence of JAWS and PJVS systems.

6.2. AC stepwise to ac stepwise comparisons

Direct comparisons between two stepwise approximated PJVS waveforms [120, 133] provide useful information regarding the accuracy of voltage steps and verify that the proper method to remove transients has been applied. If the two PJVS arrays to be compared have different designs or are biased at different microwave frequencies, then the residual voltage δV_i for each step of the waveform will be in the range $-V_{\mathrm{LSB}}/2 < \delta V_i < V_{\mathrm{LSB}}/2$, with V_{LSB} being the largest LSB voltage of the two PJVS arrays [120]. Therefore, reaching a perfect cancellation between two waveforms is not guaranteed. A 10 nV V^{-1} relative agreement between two stepwise waveforms was measured for frequencies $<$60 Hz [120]. The accuracy of the comparison is ultimately limited by the stability, noise, non-linearity and gain error of the digitizer used to measure the differential voltage. Because JAWS systems can generate stepwise-approximated waveforms, this comparison method can also be applied to JAWS-PJVS comparisons. Even if this method does not exploit the lack of inherently non-quantized transients in JAWS, this type of comparison may provide a useful tool to test the measurement setup and the digitizer.

The measured agreement between two stepwise approximated waveforms remains an abstract concept. It is misleading to quote the result of this comparison measurement as a specification for a PJVS system, because the measurement is not applicable to any ac voltage metrology application. For example, the measurement does not account for any of the errors associated with rms values of an ac source, as discussed in previous sections.

6.3. Direct ac sinewave to ac stepwise comparisons

Comparing JAWS sinewaves to PJVS stepwise-approximated waveforms is probably the most interesting and challenging method to verify the equivalence of these systems. The first direct JAWS-to-PJVS comparison was performed at 100 mV and 500 Hz with a sampling and multiplexing method and reported a relative agreement of (-0.18 ± 0.26) μV V^{-1} [165]. A lower relative uncertainty of $(+3.5 \pm 11.7)$ nV V^{-1} was achieved at 1 V and 250 Hz with a differential sampling method [49]. This type of comparison is an ideal tool to test the limits of the differential sampling method and to quantify the magnitude of potential systematic errors associated with the JAWS or the PJVS. Unfortunately, the overlap between the two types of JVS systems (see figure 13) is limited by the JAWS output voltage (presently $\leqslant$2 V rms) and the range of the PJVS stepwise waveform frequency ($\leqslant$1 kHz).

6.4. Direct ac sinewave to ac sinewave comparisons

Direct comparison of two sinewaves can be achieved by connecting two JAWS arrays in series and applying a relative phase shift of 180° between the two waveforms. This type of comparison requires synchronization and fine adjustment of the relative phase between the two waveforms to null the differential voltage. Fine phase adjustment is achieved by rotating the pulse pattern of one waveform by one or multiple clock cycles of the pulse generator. The residual voltage can be either measured with a lock-in amplifier at the frequency of the sinewaves [167] or with a digitizer [164]. Like the ac sinewave to ac stepwise comparison, JAWS-to-JAWS comparisons provide the high resolution needed to perform QLR characterization of bias parameters. As an example, such QLR measurements would be useful to characterize systematic errors that scale with the frequency of JAWS sinewave and errors that are due to the ac leakage current.

6.5. Indirect comparison measurements

Another way to link two JVS systems is through indirect comparison measurements. Such comparisons require using an ac source with a good short-term amplitude stability as a transfer standard (see section 5). The indirect comparisons that can be applied to JAWS and PJVS systems are represented by the four diagonal arrows in figure 14. At least two measurements performed in quick succession are required to establish equivalence between two JVS systems. The main advantage of this method is its ability to verify that proper measurement and analysis methods have been applied to transfer the accuracy of the JVS to the ac source. The measured uncertainty will not be as small as with a direct JVS comparison, because the transferring ac source is not an intrinsic standard. However, if the amplitude of the ac source can be predicted with a long-term uncertainty of 1 μV V^{-1} or less, then it can be implemented as a traveling standard and can be used in 'round-robin' interlaboratory comparisons (ILC). Establishing verification of ac voltage measurement capability through a transfer-standard ILC would simplify logistics compared to performing on-site JVS comparisons. dc voltage ILCs with a Zener traveling reference are periodically conducted in North America [176].

6.6. SI redefinition impact

The proposed redefinition of the SI will impact the voltage metrology community far beyond a simple change in terminology from 'representation' to 'realization' and a shift in the numerical values of the fundamental constants e and h. After the redefinition, traceability will be replaced with verification because *every* JVS system will realize the unit volt and not just a handful of 'gold standard' JVS systems at NMIs. The role of the NMIs will shift from providing a traceable JVS reference to verifying that the disseminated JVS systems are functioning

correctly. The biggest impact of the SI redefinition may be on ac voltage metrology. JAWS and PJVS waveforms, with a direct link to the SI, provide a strong motivation to switch from detector-based to source-based ac voltage metrology. The success of this paradigm shift depends on development of new commercial ac sources that can perform as secondary references. Additional research on direct comparison of JAWS and PJVS waveforms is needed to characterize all potential sources of error, followed by establishing the measurement protocol for ac voltage comparisons.

7. Conclusion

This review article describes in detail the presently fabricated PJVS and JAWS devices, systems and measurement capabilities, as well as their performance and the systematic errors associated with their different voltage generation methods. PJVS and JAWS are increasingly implemented in numerous applications and calibrations, for both dc and ac voltage metrology. By employing full automation and cryocooled refrigeration, the dissemination of quantum voltage standards is expanding beyond NMI laboratories and into secondary and industrial calibration laboratories. After the SI redefinition, PJVS and JAWS systems will, in practice, directly realize the unit volt in all laboratories. JAWS systems have huge potential for continued development, including further increases in output voltage through design of more complex circuits, increasing the output waveform frequency above 1 MHz, and by applying new bias techniques. In the future, electricity, mass, and temperature metrology and commercial instruments will largely benefit from the order of magnitude improvement in the stability, programmability, linearity and accuracy provided by ac JVS sources.

Acknowledgment

The authors thank J Brevik, C Burroughs, G Butler, P Dresselhaus, A Fox, D Olaya, R Schwall, and S Waltman in the NIST Quantum Voltage Project for their contributions to the development, fabrication and evaluation of the NIST JVS circuits as well as our collaborators S Cular, D Haddad, T Lipe, T Nelson, F Seiffert, Y Tang, W Tew, J Underwood, and B Waltrip for the implementation of JVS metrology applications at the NIST Gaithersburg campus. They would also like to thank Hirotake Yamamori, Oliver Kieler, and Johannes Kohlmann for their kind permission to present the picture of their devices in the figures.

ORCID iDs

Alain Rüfenacht https://orcid.org/0000-0002-1579-9738
Nathan E Flowers-Jacobs https://orcid.org/0000-0002-9081-5187
Samuel P Benz https://orcid.org/0000-0002-8679-0765

References

[1] Josephson B D 1962 Possible new effects in superconductive tunnelling *Phys. Lett.* **1** 251–3
[2] Hamilton C A 2000 Josephson voltage standards *Rev. Sci. Instrum.* **71** 3611
[3] Jeanneret B and Benz S P 2009 Application of the Josephson effect in electrical metrology *Eur. Phys. J. Spec. Top.* **172** 181–206
[4] Benz S P 1995 Superconductor-normal-superconductor junctions for programmable voltage standards *Appl. Phys. Lett.* **6711** 2714
[5] Hamilton C A, Burroughs C J and Kautz R L 1995 Josephson D/A converter with fundamental accuracy *IEEE Trans. Instrum. Meas.* **44** 223–5
[6] CGPM 2014 *Resolution 1 of the 25th Meeting of the CGPM General Conf. on Weights and Measures, 2014 (Versailles)* (www.bipm.org/utils/common/pdf/CGPM-2014/25th-CGPM-Resolutions.pdf)
[7] Consultative Committees of the CIPM 2017 Information for users about the proposed revision of the SI (www.bipm.org/utils/common/pdf/SI-statement.pdf)
[8] Djordjevic S, Séron O, Solve S and Chayramy R 2008 Direct comparison between a programmable and a conventional Josephson voltage standard at the level of 10 V *Metrologia* **45** 429–35
[9] Tang Y, Ojha V N, Schlamminger S, Rüfenacht A, Burroughs C J, Dresselhaus P D and Benz S P 2012 A 10 V programmable Josephson voltage standard and its applications for voltage metrology *Metrologia* **49** 635–43
[10] Rüfenacht A, Tang Y, Solve S, Fox A E, Dresselhaus P D, Burroughs C J, Schwall R E, Chayramy R and Benz S P 2018 Automated direct comparison of two cryocooled 10 V programmable Josephson voltage standards *Metrologia* **55** 585–96
[11] Inglis B D 1992 Standards for AC–DC transfer *Metrologia* **29** 191–9
[12] Kieler O F, Behr R, Wendisch R, Bauer S, Palafox L and Kohlmann J 2015 Towards a 1 V Josephson arbitrary waveform synthesizer *IEEE Trans. Appl. Supercond.* **25** 1–5
[13] Flowers-Jacobs N E, Fox A E, Dresselhaus P D, Schwall R E and Benz S P 2016 Two-Volt Josephson arbitrary waveform synthesizer using wilkinson dividers *IEEE Trans. Appl. Supercond.* **26** 1–7
[14] Flowers-Jacobs N E, Waltman S B, Fox A E, Dresselhaus P D and Benz S P 2016 Josephson arbitrary waveform synthesizer with two layers of wilkinson dividers and an FIR filter *IEEE Trans. Appl. Supercond.* **26** 1–7
[15] Shapiro S 1963 Josephson currents in superconducting tunneling: the effect of microwaves and other observations *Phys. Rev. Lett.* **11** 80–2
[16] Quinn T J 1989 News from the BIPM *Metrologia* **26** 69–74
[17] Newell D B *et al* 2018 The CODATA 2017 values of h, e, k, and N_A for the revision of the SI *Metrologia* **55** L13–6
[18] Burroughs C J, Dresselhaus P D, Rüfenacht A, Olaya D, Elsbury M M, Tang Y-H and Benz S P 2011 NIST 10 V Programmable Josephson voltage standard system *IEEE Trans. Instrum. Meas.* **60** 2482–8
[19] Behr R, Kieler O, Kohlmann J, Müller F and Palafox L 2012 Development and metrological applications of Josephson arrays at PTB *Meas. Sci. Technol.* **23** 124002
[20] Burroughs C J, Benz S P, Hamilton C A and Harvey T E 1999 Programmable 1 V dc voltage standard *IEEE Trans. Instrum. Meas.* **48** 279–81
[21] Behr R, Grimm L, Funck T, Kohlmann J, Schulze H, Muller F, Schumacher B, Warnecke P and Niemeyer J 2001

Application of Josephson series arrays to a DC quantum voltmeter *IEEE Trans. Instrum. Meas.* **50** 185–7
[22] Chong Y, Burroughs C J, Dresselhaus P D, Hadacek N, Yamamori H and Benz S P 2005 2.6 V high-resolution programmable Josephson voltage standard circuits using double-stacked $MoSi_2$-barrier junctions *IEEE Trans. Instrum. Meas.* **54** 616–9
[23] Baek B, Dresselhaus P D and Benz S P 2006 Co-sputtered amorphous Nb_xSi_{1-x} barriers for Josephson-junction circuits *IEEE Trans. Appl. Supercond.* **16** 1966–70
[24] Dresselhaus P D, Elsbury M M, Olaya D, Burroughs C J and Benz S P 2011 10 V programmable Josephson voltage standard circuits using NbSi-barrier junctions *IEEE Trans. Appl. Supercond.* **21** 693–6
[25] Elsbury M M, Dresselhaus P D, Bergren N F, Burroughs C J, Benz S P and Popovic Z 2009 Broadband lumped-element integrated *N*-way power dividers for voltage standards *IEEE Trans. Microw. Theory Tech.* **57** 2055–63
[26] Dresselhaus P D, Elsbury M M and Benz S P 2009 Tapered Transmission Lines With Dissipative Junctions *IEEE Trans. Appl. Supercond.* **19** 993–8
[27] Chong Y, Burroughs C J, Dresselhaus P D, Hadacek N, Yamamori H and Benz S P 2005 Practical high-resolution programmable Josephson voltage standards using double- and triple- stacked $MoSi_2$-barrier junctions *IEEE Trans. Appl. Supercond.* **15** 461–4
[28] Mueller F, Behr R, Palafox L, Kohlmann J, Wendisch R and Krasnopolin I 2007 Improved 10 V SINIS series arrays for applications in AC voltage metrology *IEEE Trans. Appl. Supercond.* **17** 649–52
[29] Mueller F, Behr R, Weimann T, Palafox L, Olaya D, Dresselhaus P D and Benz S P 2009 1 V and 10 V SNS programmable voltage standards for 70 GHz *IEEE Trans. Appl. Supercond.* **19** 981–6
[30] Mueller F, Scheller T, Wendisch R, Behr R, Kieler O, Palafox L and Kohlmann J 2013 NbSi barrier junctions tuned for metrological applications up to 70 GHz: 20 V arrays for programmable Josephson voltage standards *IEEE Trans. Appl. Supercond.* **23** 1101005
[31] Yamamori H, Ishizaki M, Shoji A, Dresselhaus P D and Benz S P 2006 10 V programmable Josephson voltage standard circuits using $NbN/TiN_x/NbN/TiN_x/NbN$ double-junction stacks *Appl. Phys. Lett.* **88** 042503
[32] Yamamori H, Yamada T, Sasaki H and Shoji A 2008 A 10 V programmable Josephson voltage standard circuit with a maximum output voltage of 20 V *Supercond. Sci. Technol.* **21** 105007
[33] Yamamori H, Yamada T, Sasaki H and Shoji A 2010 Improved Fabrication Yield for 10 V programmable Josephson voltage standard circuit including 524288 NbN/TiN/NbN Josephson junctions *IEEE Trans. Appl. Supercond.* **20** 71–5
[34] Fox A E, Dresselhaus P D, Rüfenacht A, Sanders A and Benz S P 2015 Junction yield analysis for 10 V programmable Josephson voltage standard devices *IEEE Trans. Appl. Supercond.* **25** 1–5
[35] Yamamori H and Kohjiro S 2016 Fabrication of voltage standard circuits utilizing a serial-parallel power divider *IEEE Trans. Appl. Supercond.* **26** 1–4
[36] Fluke 2013 Fractional ppm traceability using your 734A/732B series DC reference standards *Fluke Calibration Application Note* (http://download.flukecal.com/pub/literature/1260304D_734A_732B_Fract_Trace_AN_w.pdf)
[37] Maruyama M, Urano C, Kaneko N, Sannomaru E, Yonezawa T, Kanai T, Yoshida H and Yoshino Y 2016 Development of a compact Zener DC voltage standard with detachable module system *2016 Conf. on Precision Electromagnetic Measurements (CPEM 2016)* (IEEE) (https://doi.org/10.1109/CPEM.2016.7540703)
[38] Lacquaniti V, De Leo N, Fretto M, Sosso A, Müller F and Kohlmann J 2011 1 V programmable voltage standards based on SNIS Josephson junction series arrays *Supercond. Sci. Technol.* **24** 045004
[39] Khorshev S K, Pashkovsky A I, Rogozhkina N V, Levichev M Y, Pestov E E, Katkov A S, Behr R, Kohlmann J and Klushin A M 2016 Accuracy of the new voltage standard using Josephson junctions cooled to 77 K *2016 Conf. on Precision Electromagnetic Measurements (CPEM 2016)* (IEEE) (https://doi.org/10.1109/CPEM.2016.7540701)
[40] Klushin A M, Pestov E E, Galin M A and Levichev M Y 2016 High-temperature superconductor Josephson junctions for voltage standards *Phys. Solid State* **58** 2196–202
[41] Hamilton C A, Burroughs C J, Benz S P and Kinard J R 1997 AC Josephson voltage standard: progress report *IEEE Trans. Instrum. Meas.* **46** 224–8
[42] Yamada T, Urano C, Nishinaka H, Murayama Y, Iwasa A, Yamamori H, Sasaki H, Shoji A and Nakamura Y 2010 Single-chip 10 V programmable Josephson voltage standard system based on a refrigerator and its precision evaluation *IEEE Trans. Appl. Supercond.* **20** 21–5
[43] Rüfenacht A, Howe L A, Fox A E, Schwall R E, Dresselhaus P D, Burroughs C J and Benz S P 2015 Cryocooled 10 V programmable Josephson voltage standard *IEEE Trans. Instrum. Meas.* **64** 1477–82
[44] Schubert M *et al* 2016 A dry-cooled AC quantum voltmeter *Supercond. Sci. Technol.* **29** 105014
[45] Benz S P and Hamilton C A 1996 A pulse-driven programmable Josephson voltage standard *Appl. Phys. Lett.* **68** 3171
[46] Candy J C 1997 An overview of basic concepts *Delta-Sigma Data Converters: Theory, Design, and Simulation* ed S R Norsworthy *et al* (Piscataway, NJ: IEEE Press)
[47] Pavan S, Schreier R and Temes G C 2017 *Understanding Delta-Sigma Data Converters* (New York: Wiley)
[48] Kohlmann J, Kieler O, Scheller T, Egeling B, Wendisch R and Behr R 2016 Series arrays of NbSi barrier Josephson junctions for AC voltage standards *2016 Conf. on Precision Electromagnetic Measurements (CPEM 2016)* (IEEE) (https://doi.org/10.1109/CPEM.2016.7540562)
[49] Behr R, Kieler O, Lee J, Bauer S, Palafox L and Kohlmann J 2015 Direct comparison of a 1 V Josephson arbitrary waveform synthesizer and an ac quantum voltmeter *Metrologia* **52** 528–37
[50] Filipski P S, van den Brom H E and Houtzager E 2012 International comparison of quantum AC voltage standards for frequencies up to 100 kHz *Measurement* **45** 2218–25
[51] van den Brom H E and Houtzager E 2012 Voltage lead corrections for a pulse-driven ac Josephson voltage standard *Meas. Sci. Technol.* **23** 124007
[52] Hagen T, Budovsky I, Benz S P and Burroughs C J 2012 Calibration system for AC measurement standards using a pulse-driven Josephson voltage standard and an inductive voltage divider *2012 Conf. on Precision Electromagnetic Measurements (CPEM 2012)* (IEEE) pp 672–3
[53] van den Brom H E, Kieler O F O, Bauer S and Houtzager E 2017 AC–DC calibrations with a pulse-driven AC Josephson voltage standard operated in a small cryostat *IEEE Trans. Instrum. Meas.* **66** 1391–6
[54] Durandetto P, Monticone E, Trinchera B, Serazio D and Sosso A 2017 Cryocooled programmable and pulse-driven Josephson voltage standards at INRiM *2017 IEEE Int. Instrumentation and Measurement Technology Conf. (I2MTC)* (IEEE) (https://doi.org/10.1109/I2MTC.2017.7969790)
[55] Benz S P, Hamilton C A, Burroughs C J and Harvey T E 1999 AC and DC bipolar voltage source using quantized pulses *IEEE Trans. Instrum. Meas.* **48** 266–9

[56] Benz S P, Burroughs C J, Harvey T E and Hamilton C A 1999 Operating conditions for a pulse-quantized AC and DC bipolar voltage source *IEEE Trans. Appl. Supercond.* **9** 3306–9
[57] Benz S P, Burroughs C J and Dresselhaus P D 2001 AC coupling technique for Josephson waveform synthesis *IEEE Trans. Appl. Supercond.* **11** 612–6
[58] van den Brom H E, Houtzager E, Brinkmeier B E R and Chevtchenko O A 2008 Bipolar pulse-drive electronics for a Josephson arbitrary waveform synthesizer *IEEE Trans. Instrum. Meas.* **57** 428–31
[59] Houtzager E, Benz S P and van den Brom H E 2009 Operating margins for a pulse-driven Josephson arbitrary waveform synthesizer using a ternary bit-stream generator *IEEE Trans. Instrum. Meas.* **58** 775–80
[60] Houtzager E, van den Brom H E and van Woerkom D 2010 Automatic tuning of the pulse-driven AC Josephson voltage standard *2010 Conf. on Precision Electromagnetic Measurements (CPEM 2010)* (IEEE) pp 185–6
[61] Benz S P and Waltman S B 2014 Pulse-bias electronics and techniques for a Josephson arbitrary waveform synthesizer *IEEE Trans. Appl. Supercond.* **24** 1–7
[62] Zhou K, Qu J and Benz S P 2015 Zero-compensation method and reduced inductive voltage error for the AC Josephson voltage standard *IEEE Trans. Appl. Supercond.* **25** 1400806
[63] Watanabe M, Dresselhaus P D and Benz S P 2006 Resonance-free low-pass filters for the AC Josephson voltage standard *IEEE Trans. Appl. Supercond.* **16** 49–53
[64] Benz S P, Waltman S B, Fox A E, Dresselhaus P D, Rüfenacht A, Underwood J M, Howe L A, Schwall R E and Burroughs C J 2015 1 V Josephson arbitrary waveform synthesizer *IEEE Trans. Appl. Supercond.* **25** 1–8
[65] Benz S P, Waltman S B, Fox A E, Dresselhaus P D, Rüfenacht A, Howe L, Schwall R E and Flowers-Jacobs N E 2015 Performance improvements for the NIST 1 V Josephson arbitrary waveform synthesizer *IEEE Trans. Appl. Supercond.* **25** 1–5
[66] Brevik J A, Flowers-Jacobs N E, Fox A E, Golden E B, Dresselhaus P D and Benz S P 2017 Josephson arbitrary waveform synthesis with multilevel pulse biasing *IEEE Trans. Appl. Supercond.* **27** 1–7
[67] Burroughs C J, Benz S P and Dresselhaus P D 2003 AC Josephson voltage standard error measurements and analysis *IEEE Trans. Instrum. Meas.* **52** 542–4
[68] Landim R P, Benz S P, Member S, Dresselhaus P D and Burroughs C J 2008 Systematic-error signals in the AC Josephson voltage standard: measurement and reduction *IEEE Trans. Instrum. Meas.* **57** 1215–20
[69] Likharev K K and Semenov V K 1991 RSFQ logic/memory family: a new Josephson-junction technology for sub-terahertz-clock-frequency digital systems *IEEE Trans. Appl. Supercond.* **1** 3–28
[70] Sasaki H, Bubanja V, Kiryu S, Hirayama F, Maezawa M and Shoji A 2001 Evaluation of AC–DC difference of thermal converters using an SFQ-based D/A converter *IEEE Trans. Instrum. Meas.* **50** 318–21
[71] Maezawa M, Mizugaki Y, Takahashi Y and Shimada H 2014 9 bit superconductive single-flux-quantum digital-to-analogue converter *Electron. Lett.* **50** 1637–9
[72] Budovsky I, Sasaki H and Coogan P 2003 AC–DC transfer comparator for the calibration of thermal voltage converters against Josephson alternating voltage standards *IEEE Trans. Instrum. Meas.* **52** 538–41
[73] Maezawa M, Yamada T and Urano C 2014 Integrated quantum voltage noise source for Johnson noise thermometry *J. Phys.: Conf. Ser.* **507** 42023
[74] Solve S, Rüfenacht A, Burroughs C J and Benz S P 2013 Direct comparison of two NIST PJVS systems at 10 V *Metrologia* **50** 441–51
[75] Eichenberger A, Baumann H, Jeanneret B, Jeckelmann B, Richard P and Beer W 2011 Determination of the Planck constant with the METAS watt balance *Metrologia* **48** 133–41
[76] Fang H, Kiss A, Picard A and Stock M 2014 A watt balance based on a simultaneous measurement scheme *Metrologia* **51** S80–7
[77] Haddad D, Seifert F, Chao L S, Possolo A, Newell D B, Pratt J R, Williams C J and Schlamminger S 2017 Measurement of the Planck constant at the National Institute of Standards and Technology from 2015 to 2017 *Metrologia* **54** 633–41
[78] Wood B M, Sanchez C A, Green R G and Liard J O 2017 A summary of the Planck constant determinations using the NRC Kibble balance *Metrologia* **54** 399–409
[79] Thomas M, Ziane D, Pinot P, Karcher R, Imanaliev A, Dos Santos F P, Merlet S, Piquemal F and Espel P 2017 A determination of the Planck constant using the LNE Kibble balance in air *Metrologia* **54** 468–80
[80] Li Z *et al* 2017 The first determination of the Planck constant with the joule balance NIM-2 *Metrologia* **54** 763–74
[81] Lombardi M A 2016 Evaluating the frequency and time uncertainty of GPS disciplined oscillators and clocks *NCSLI Meas.* **11** 30–44
[82] Williams J M, Henderson D, Patel P, Behr R and Palafox L 2007 Achieving Sub-100 ns switching of programmable Josephson arrays *IEEE Trans. Instrum. Meas.* **56** 651–4
[83] Seron O, Djordjevic S, Budovsky I, Hagen T, Behr R and Palafox L 2012 Precision AC–DC transfer measurements with a Josephson waveform synthesizer and a buffer amplifier *IEEE Trans. Instrum. Meas.* **61** 198–204
[84] Budovsky I, Behr R, Palafox L, Djordjevic S and Hagen T 2012 Technique for the calibration of thermal voltage converters using a Josephson waveform synthesizer and a transconductance amplifier *Meas. Sci. Technol.* **23** 124005
[85] Burroughs C J, Rüfenacht A, Benz S P, Dresselhaus P D, Waltrip B C and Nelson T L 2008 Error and transient analysis of stepwise-approximated sine waves generated by programmable Josephson voltage standards *IEEE Trans. Instrum. Meas.* **57** 1322–9
[86] Burroughs C J, Rüfenacht A, Benz S P and Dresselhaus P D 2009 Systematic error analysis of stepwise-approximated AC waveforms generated by programmable Josephson voltage standards *IEEE Trans. Instrum. Meas.* **58** 761–7
[87] Helisto P, Nissila J, Ojasalo K, Penttila J S and Seppa H 2003 AC voltage standard based on a programmable SIS array *IEEE Trans. Instrum. Meas.* **52** 533–7
[88] Behr R, Williams J M, Patel P, Janssen T J B M, Funck T and Klonz M 2005 Synthesis of precision waveforms using a SINIS Josephson junction array *IEEE Trans. Instrum. Meas.* **54** 612–5
[89] Burroughs C J *et al* 2007 Development of a 60 Hz power standard using SNS programmable Josephson voltage standards *IEEE Trans. Instrum. Meas.* **56** 289–94
[90] Lee J, Schurr J, Nissilä J, Palafox L and Behr R 2010 The Josephson two-terminal-pair impedance bridge *Metrologia* **47** 453–9
[91] Lee J, Schurr J, Nissilä J, Palafox L, Behr R and Kibble B P 2011 Programmable Josephson arrays for impedance measurements *IEEE Trans. Instrum. Meas.* **60** 2596–601
[92] Budovsky I, Georgakopoulos D, Hagen T, Sasaki H and Yamamori H 2011 Precision AC–DC difference measurement system based on a programmable Josephson voltage standard *IEEE Trans. Instrum. Meas.* **60** 2439–44
[93] Palafox L, Behr R, Nissila J, Schurr J and Kibble B P 2012 Josephson impedance bridges as universal impedance comparators *2012 Conf. on Precision Electromagnetic Measurements* (IEEE) pp 464–5

[94] Behr R, Kieler O F O, Schleubner D, Palafox L and Ahlers F-J 2013 Combining Josephson systems for spectrally pure AC waveforms with large amplitudes *IEEE Trans. Instrum. Meas.* **62** 1634–9

[95] Palafox L, Behr R, Schurr J and Kibble B P 2014 Precision 10:1 capacitance ratio measurement using a Josephson impedance bridge *2014 Conf. on Precision Electromagnetic Measurements (CPEM 2014)* (IEEE) pp 232–3

[96] Eklund G, Bergsten T, Hagen T, Palafox L and Behr R 2016 A comparison of the Josephson impedance bridges of PTB and SP *2016 Conf. on Precision Electromagnetic Measurements (CPEM 2016)* (IEEE) (https://doi.org/10.1109/CPEM.2016.7540584)

[97] Hagen T, Thevenot O, Seron O, Khan S, Palafox L and Behr R 2016 Comparison of the frequency dependence of capacitance ratios between LNE and PTB *2016 Conf. on Precision Electromagnetic Measurements (CPEM 2016)* (IEEE) (https://doi.org/10.1109/CPEM.2016.7540585)

[98] Hagen T, Palafox L and Behr R 2017 A Josephson impedance bridge based on programmable Josephson voltage standards *IEEE Trans. Instrum. Meas.* **66** 1539–45

[99] Jeanneret B, Overney F, Callegaro L, Mortara A and Rüfenacht A 2009 Josephson-voltage-standard-locked sine wave synthesizer: margin evaluation and stability *IEEE Trans. Instrum. Meas.* **58** 791–6

[100] Jeanneret B, Overney F, Rüfenacht A and Nissila J 2010 Strong attenuation of the transients' effect in square waves synthesized with a programmable Josephson voltage standard *IEEE Trans. Instrum. Meas.* **59** 1894–9

[101] Burroughs C J, Benz S P, Hamilton C A, Harvey T E, Kinard J R, Lipe T E and Sasaki H 1999 Thermoelectric transfer difference of thermal converters measured with a Josephson source *IEEE Trans. Instrum. Meas.* **48** 282–4

[102] Funck T, Behr R and Klonz M 2001 Fast reversed DC measurements on thermal converters using a SINIS Josephson junction array *IEEE Trans. Instrum. Meas.* **50** 322–5

[103] Eklund G, Bergsten T, Tarasso V and Rydler K-E 2011 Determination of transition error corrections for low frequency stepwise-approximated Josephson sine waves *IEEE Trans. Instrum. Meas.* **60** 2399–403

[104] Burroughs C J, Rüfenacht A, Benz S P and Dresselhaus P D 2013 Method for ensuring accurate AC waveforms with programmable Josephson voltage standards *IEEE Trans. Instrum. Meas.* **62** 1627–33

[105] Filipski P S, Kinard J R, Lipe T E and Benz S P 2009 Correction of systematic errors due to the voltage leads in an AC Josephson voltage standard *IEEE Trans. Instrum. Meas.* **58** 853–8

[106] Filipski P S, Boecker M, Benz S P and Burroughs C J 2011 Experimental determination of the voltage lead error in an AC Josephson voltage standard *IEEE Trans. Instrum. Meas.* **60** 2387–92

[107] van den Brom H E, Zhao D and Houtzager E 2016 Voltage lead errors in an AC Josephson voltage standard: explanation in terms of standing waves *2016 Conf. on Precision Electromagnetic Measurements (CPEM 2016)* (IEEE) (https://doi.org/10.1109/CPEM.2016.7540666)

[108] Zhao D, van den Brom H E and Houtzager E 2017 Mitigating voltage lead errors of an AC Josephson voltage standard by impedance matching *Meas. Sci. Technol.* **28** 95004

[109] Underwood J M 2018 Uncertainty analysis for ac–dc difference measurements with the AC Josephson voltage standard in preparation

[110] Lipe T E, Kinard J R, Tang Y, Benz S P, Burroughs C J and Dresselhaus P D 2008 Thermal voltage converter calibrations using a quantum ac standard *Metrologia* **45** 275–80

[111] Maruyama M, Iwasa A, Yamamori H, Chen S-F, Urano C and Kaneko N 2015 Calibration system for zener voltage standards using a 10 V programmable Josephson voltage standard at NMIJ *IEEE Trans. Instrum. Meas.* **64** 1606–12

[112] Witt T J 2002 Maintenance and dissemination of voltage standards by Zener-diode-based instruments *IEE Proc., Sci. Meas. Technol.* **149** 305–12

[113] Hamilton C A and Tarr L W 2003 Projecting Zener dc reference performance between calibrations *IEEE Trans. Instrum. Meas.* **52** 454–6

[114] van den Brom H E, Houtzager E, Rietveld G, van Bemmelen R and Chevtchenko O 2007 Voltage linearity measurements using a binary Josephson system *Meas. Sci. Technol.* **18** 3316–20

[115] Maruyama M, Takahashi H, Katayama K, Yonezawa T, Kanai T, Iwasa A, Urano C, Kiryu S and Kaneko N 2015 Evaluation of linearity characteristics in digital voltmeters using a PJVS system With a 10 K cooler *IEEE Trans. Instrum. Meas.* **64** 1613–9

[116] Rüfenacht A, Burroughs C J, Benz S P and Dresselhaus P D 2012 A digital-to-analog converter with a voltage standard reference *2012 Conf. on Precision Electromagnetic Measurements (CPEM 2012)* (IEEE) pp 436–7

[117] Tang Y, Bartel T W and Sims J E 2008 Ratio calibration of a digital voltmeter for force measurement using the programmable Josephson voltage standard *NCSLI Meas.* **3** 70–5

[118] Rüfenacht A, Fox A E, Dresselhaus P D, Burroughs C J, Benz S P, Waltrip B C and Nelson T L 2016 Simultaneous double waveform synthesis with a single programmable Josephson voltage standard *2016 Conf. on Precision Electromagnetic Measurements (CPEM 2016)* (IEEE) (https://doi.org/10.1109/CPEM.2016.7540471)

[119] Chong Y, Kim M S and Kim K T 2006 Fast and almost continuously programmable Josephson voltage standard system with multiple microwave drive *2006 Conf. on Precision Electromagnetic Measurements (CPEM 2006) Conf. Digest* pp 382–3

[120] Rüfenacht A, Burroughs C J and Benz S P 2008 Precision sampling measurements using ac programmable Josephson voltage standards *Rev. Sci. Instrum.* **79** 044704

[121] Georgakopoulos D, Budovsky I, Hagen T, Sasaki H and Yamamori H 2012 Dual radiofrequency drive quantum voltage standard with nanovolt resolution based on a closed-loop refrigeration cycle *Meas. Sci. Technol.* **23** 124003

[122] Li H, Gao Y and Wang Z 2016 A differential programmable Josephson voltage standard for low-measurement *2016 Conf. on Precision Electromagnetic Measurements (CPEM 2016)* (IEEE) (https://doi.org/10.1109/CPEM.2016.7540473)

[123] Solve S, Chayramy R, Maruyama M, Urano C, Kaneko N-H and Rüfenacht A 2018 Direct DC 10 V comparison between two programmable Josephson voltage standards made of niobium nitride (NbN)-based and niobium (Nb)-based Josephson junctions *Metrologia* **55** 302–13

[124] Behr R, Kieler O and Schumacher B 2017 A precision microvolt-synthesizer based on a pulse-driven Josephson voltage standard *IEEE Trans. Instrum. Meas.* **66** 1385–90

[125] Robinson I A and Schlamminger S 2016 The watt or Kibble balance: a technique for implementing the new SI definition of the unit of mass *Metrologia* **53** A46–74

[126] Devoille L, Feltin N, Steck B, Chenaud B, Sassine S, Djordevic S, Séron O and Piquemal F 2012 Quantum metrological triangle experiment at LNE: measurements on a three-junction R-pump using a 20 000:1 winding ratio cryogenic current comparator *Meas. Sci. Technol.* **23** 124011

[127] Scherer H and Camarota B 2012 Quantum metrology triangle experiments: a status review *Meas. Sci. Technol.* **23** 124010

[128] Brun-Picard J, Djordjevic S, Leprat D, Schopfer F and Poirier W 2016 Practical quantum realization of the ampere from the elementary charge *Phys. Rev.* X **6** 041051
[129] Lee J, Behr R, Schumacher B, Palafox L, Schubert M, Starkloff M, Bock A C and Fleischmann P M 2016 From AC quantum voltmeter to quantum calibrator *2016 Conf. on Precision Electromagnetic Measurements (CPEM 2016)* (IEEE) (https://doi.org/10.1109/CPEM.2016.7540470)
[130] Palafox L, Ramm G, Behr R, Kurten Ihlenfeld W G and Moser H 2007 Primary AC power standard based on programmable Josephson junction arrays *IEEE Trans. Instrum. Meas.* **56** 534–7
[131] Rüfenacht A, Overney F, Mortara A and Jeanneret B 2011 Thermal-transfer standard validation of the Josephson-voltage-standard-locked sine-wave synthesizer *IEEE Trans. Instrum. Meas.* **60** 2372–7
[132] Jeanneret B, Overney F and Rüfenacht A 2012 The Josephson locked synthesizer *Meas. Sci. Technol.* **23** 124004
[133] Behr R, Palafox L, Ramm G, Moser H and Melcher J 2007 Direct comparison of Josephson waveforms using an AC quantum voltmeter *IEEE Trans. Instrum. Meas.* **56** 235–8
[134] Rüfenacht A, Burroughs C J, Benz S P, Dresselhaus P D, Waltrip B C and Nelson T L 2009 Precision differential sampling measurements of low-frequency synthesized sine waves with an AC programmable Josephson voltage standard *IEEE Trans. Instrum. Meas.* **58** 809–15
[135] Kim M-S, Kim K-T, Kim W-S, Chong Y and Kwon S-W 2010 Analog-to-digital conversion for low-frequency waveforms based on the Josephson voltage standard *Meas. Sci. Technol.* **21** 115102
[136] Williams J M, Henderson D, Pickering J, Behr R, Müller F and Scheibenreiter P 2011 Quantum-referenced voltage waveform synthesiser *IET Sci. Meas. Technol.* **5** 163–74
[137] Amagai Y, Maruyama M and Fujiki H 2013 Low-frequency characterization in thermal converters using AC-programmable Josephson voltage standard system *IEEE Trans. Instrum. Meas.* **62** 1621–6
[138] Kurten Ihlenfeld W G and Pinheiro Landim R 2015 An automated Josephson-based AC-voltage calibration system *IEEE Trans. Instrum. Meas.* **64** 1779–84
[139] Wang Z, Li H, Yang Y and Gao Y 2016 Research on differential sampling with a Josephson voltage standard *2016 Conf. on Precision Electromagnetic Measurements (CPEM 2016)* (IEEE) pp 1–2
[140] Rüfenacht A, Burroughs C J, Dresselhaus P D and Benz S P 2013 Differential sampling measurement of a 7 V RMS sine wave with a programmable Josephson voltage standard *IEEE Trans. Instrum. Meas.* **62** 1587–93
[141] Lee J, Behr R, Palafox L, Katkov A, Schubert M, Starkloff M and Böck A C 2013 An ac quantum voltmeter based on a 10 V programmable Josephson array *Metrologia* **50** 612–22
[142] Schubert M, Starkloff M, Lee J, Behr R, Palafox L, Wintermeier A, Boeck A C, Fleischmann P M and May T 2015 An AC josephson voltage standard up to the kilohertz range tested in a calibration laboratory *IEEE Trans. Instrum. Meas.* **64** 1620–6
[143] Chen S-F, Amagai Y, Maruyama M and Kaneko N 2015 Uncertainty evaluation of a 10 V RMS sampling measurement system using the AC programmable josephson voltage standard *IEEE Trans. Instrum. Meas.* **64** 3308–14
[144] Amagai Y, Maruyama M, Shimazaki T, Yamamori H, Fujiki H and Kaneko N 2016 Characterization of high-stability AC source using AC-programmable Josephson voltage standard system *2016 Conf. on Precision Electromagnetic Measurements (CPEM 2016)* (IEEE) (https://doi.org/10.1109/CPEM.2016.7540720)
[145] Kurten Ihlenfeld W G, Mohns E, Behr R, Williams J M, Patel P, Ramm G and Bachmair H 2005 Characterization of a high-resolution analog-to-digital converter with a Josephson AC voltage source *IEEE Trans. Instrum. Meas.* **54** 649–52
[146] Ihlenfeld W G K and Landim R P 2016 Investigations on extending the frequency range of PJVS based AC voltage calibrations by coherent subsampling *2016 Conf. on Precision Electromagnetic Measurements (CPEM 2016)* (IEEE) (https://doi.org/10.1109/CPEM.2016.7539732)
[147] Katkov A, Gubler G, Lee J, Behr R and Nissila J 2014 Influence of harmonics on AC measurements using a quantum voltmeter *2014 Conf. on Precision Electromagnetic Measurements (CPEM 2014)* (IEEE) pp 526–7
[148] Lee J, Nissila J, Katkov A and Behr R 2014 A quantum voltmeter for precision AC measurements *2014 Conf. on Precision Electromagnetic Measurements (CPEM 2014)* (IEEE) pp 732–3
[149] Waltrip B C, Gong B, Nelson T L, Wang Y, Burroughs C J, Rüfenacht A, Benz S P and Dresselhaus P D 2009 AC power standard using a programmable Josephson voltage standard *IEEE Trans. Instrum. Meas.* **58** 1041–8
[150] Overney F, Rüfenacht A, Braun J-P, Jeanneret B and Wright P S 2011 Characterization of metrological grade analog-to-digital converters using a programmable Josephson voltage standard *IEEE Trans. Instrum. Meas.* **60** 2172–7
[151] Benz S P, Burroughs C J, Dresselhaus P D and Christian L A 2001 AC and DC voltages from a Josephson arbitrary waveform synthesizer *IEEE Trans. Instrum. Meas.* **50** 181–4
[152] Benz S P, Burroughs C J, Dresselhaus P D, Lipe T E and Kinard J R 2006 100 mV AC–DC transfer standard measurements using an AC Josephson voltage standard *NCSLI Meas. J. Meas. Sci.* **1** 50–5
[153] Karlsen B, Lind K, Malmbekk H and Ohlckers P 2016 Development of high precision voltage dividers and buffer for AC voltage metrology up to 1 MHz *2016 Conf. on Precision Electromagnetic Measurements (CPEM 2016)* (IEEE) (https://doi.org/10.1109/CPEM.2016.7540456)
[154] Budovsky I and Palafox L 2016 10 V transconductance amplifier for the comparison of Josephson standards and thermal converters *2016 Conf. on Precision Electromagnetic Measurements (CPEM 2016)* (IEEE) (https://doi.org/10.1109/CPEM.2016.7540632)
[155] Palafox L, Behr R, Kieler O, Lee J, Budovsky I, Bauer S and Hagen T 2016 First metrological applications of the PTB 1 V Josephson arbitrary waveform synthesizer *2016 Conf. on Precision Electromagnetic Measurements (CPEM 2016)* (IEEE) (https://doi.org/10.1109/CPEM.2016.7540602)
[156] Toonen R C and Benz S P 2009 Non-linear behavior of electronic components characterized with precision multitones from a Josephson arbitrary waveform synthesizer *IEEE Trans. Appl. Supercond.* **19** 715–8
[157] Benz S P, Dresselhaus P D, Tew W L, White D R and Martinis J M 2003 Johnson noise thermometry measurements using a quantized voltage noise source for calibration *IEEE Trans. Instrum. Meas.* **52** 550–4
[158] White D R and Benz S P 2008 Constraints on a synthetic-noise source for Johnson noise thermometry *Metrologia* **45** 93–101
[159] Qu J, Benz S P, Coakley K, Rogalla H, Tew W L, White R, Zhou K and Zhou Z 2017 An improved electronic determination of the Boltzmann constant by Johnson noise thermometry *Metrologia* **54** 549–58

[160] Urano C, Yamazawa K and Kaneko N-H 2017 Measurement of the Boltzmann constant by Johnson noise thermometry using a superconducting integrated circuit *Metrologia* **54** 847–55

[161] Flowers-Jacobs N E, Pollarolo A, Coakley K J, Fox A E, Rogalla H, Tew W L and Benz S P 2017 A Boltzmann constant determination based on Johnson noise thermometry *Metrologia* **54** 730–7

[162] Bauer S, Behr R, Hagen T, Kieler O, Lee J, Palafox L and Schurr J 2017 A novel two-terminal-pair pulse-driven Josephson impedance bridge linking a 10 nF capacitance standard to the quantized Hall resistance *Metrologia* **54** 152–60

[163] Overney F, Flowers-Jacobs N E, Jeanneret B, Rüfenacht A, Fox A E, Underwood J M, Koffman A D and Benz S P 2016 Josephson-based full digital bridge for high-accuracy impedance comparisons *Metrologia* **53** 1045–53

[164] Flowers-Jacobs N E, Rüfenacht A, Fox A E, Dresselhaus P D and Benz S P 2016 2 V pulse-driven Josephson arbitrary waveform synthesizer *2016 Conf. on Precision Electromagnetic Measurements (CPEM 2016)* (IEEE) (https://doi.org/10.1109/CPEM.2016.7540601)

[165] Jeanneret B, Rüfenacht A, Overney F, Van Den Brom H and Houtzager E 2011 High precision comparison between a programmable and a pulse-driven Josephson voltage standard *Metrologia* **48** 311–6

[166] Rüfenacht A, Flowers-Jacobs N E, Fox A E, Burroughs C J, Dresselhaus P D and Benz S P 2016 Direct comparison of a pulse-driven Josephson arbitrary waveform synthesizer and a programmable Josephson voltage standard at 1 V *2016 Conf. on Precision Electromagnetic Measurements (CPEM 2016)* (IEEE) (https://doi.org/10.1109/CPEM.2016.7540603)

[167] Kieler O F, Behr R, Schleussner D, Palafox L and Kohlmann J 2013 Precision comparison of sine waveforms with pulse-driven Josephson arrays *IEEE Trans. Appl. Supercond.* **23** 1301404

[168] Nissila J, Sira M, Lee J, Ozturk T, Arifovic M, de Aguilar J D, Lapuh R and Behr R 2016 Stable arbitrary waveform generator as a transfer standard for ADC calibration *2016 Conf. on Precision Electromagnetic Measurements (CPEM 2016)* (IEEE) (https://doi.org/10.1109/CPEM.2016.7540454)

[169] Hamilton C A 2001 *NCSLI Recommended Intrinsic Derived Standards Practices—1 (RISP-1): Josephson Voltage Standard* 4th edn (Boulder, CO : NCSLI)

[170] Solve S 2012 Protocol of direct on-site Josephson voltage standard comparisons: BIPM.EM-K10.b (http://kcdb.bipm.org/appendixB/appbresults/BIPM.EM-K10/BIPM.EM-K10_Technical_Protocol_option_A.pdf)

[171] Solve S and Stock M 2012 BIPM direct on-site Josephson voltage standard comparisons: 20 years of results *Meas. Sci. Technol.* **23** 124001

[172] Yamada T, Urano C, Nishinaka H, Murayama Y, Iwasa A, Yamamori H, Sasaki H, Shoji A and Nakamura Y 2009 A direct comparison of a 10 V Josephson voltage standard between a refrigerator-based multi-chip programmable system and a conventional system *Supercond. Sci. Technol.* **22** 095010

[173] Honghui L, Yuan G and Zengmin W 2015 Comparison of the 10 V josephson voltage standards of the conventional and the programmable at NIM *2015 12th Int. Conf. on Electronic Measurement & Instruments (ICEMI)* (IEEE) pp 713–7

[174] Tang Y-H, Wachter J, Rüfenacht A, FitzPatrick G J and Benz S P 2015 Application of a 10 V programmable Josephson voltage standard in direct comparison with conventional Josephson voltage standards *IEEE Trans. Instrum. Meas.* **64** 3458–66

[175] Rüfenacht A, Flowers-Jacobs N, Fox A E, Waltman S B, Schwall R E, Burroughs C J, Dresselhaus P D and Benz S P 2018 DC comparison of a programmable Josephson voltage standard and a Josephson arbitrary waveform synthesizer *2018 Conf. on Precision Electromagnetic Measurements (CPEM 2018)* (IEEE) submitted

[176] Parks H V, Tang Y, Reese P, Gust J and Novak J J 2013 The North American Josephson voltage interlaboratory comparison *IEEE Trans. Instrum. Meas.* **62** 1608–14